The Journal of Chemical Physics

Cluster perturbation theory. I. Theoretical foundation for a coupled cluster target state and ground-state energies

Cite as: J. Chem. Phys. **150**, 134108 (2019); https://doi.org/10.1063/1.5004037
Submitted: 10 September 2017 . Accepted: 24 October 2018 . Published Online: 04 April 2019

Filip Pawłowski, Jeppe Olsen, and Poul Jørgensen

AIP Publishing

The Journal of Chemical Physics ARTICLE scitation.org/journal/jcp

Cluster perturbation theory. I. Theoretical foundation for a coupled cluster target state and ground-state energies

Cite as: J. Chem. Phys. 150, 134108 (2019); doi: 10.1063/1.5004037
Submitted: 10 September 2017 • Accepted: 24 October 2018 •
Published Online: 4 April 2019

Filip Pawłowski,[1,a)] Jeppe Olsen,[2] and Poul Jørgensen[2]

AFFILIATIONS

[1] Department of Chemistry and Biochemistry, Auburn University, Auburn, Alabama 36849-5312, USA
[2] Department of Chemistry, qLEAP Center for Theoretical Chemistry, Aarhus University, Langelandsgade 140, DK-8000 Aarhus C, Denmark

[a)] **Electronic mail:** filip.pawlowski1@gmail.com

ABSTRACT

We introduce a new class of perturbation models—the cluster perturbation (CP) models—where the major drawbacks of Møller-Plesset perturbation theory and coupled cluster perturbation theory have been eliminated. In CP theory, we consider a target excitation space relative to the Hartree-Fock state and partition the target excitation space into a parent and an auxiliary excitation space. The zeroth-order state is a coupled cluster (CC) state in the parent excitation space, and the target state is either a cluster linear or a CC state in the target excitation space. In CP theory, perturbation series are determined in orders of the CC parent state similarity-transformed fluctuation potential for the energy and for a molecular property, where the zeroth-order term in the series is the energy or a molecular property for the CC parent state and where the series formally converge to the energy or a molecular property for the target state. In CP theory, we use a generalized order concept, where the zeroth-order component of the extended parent-state Jacobian contains a fluctuation potential contribution, and use this new generalized order to treat internal relaxation in the parent excitation space at zeroth order and hence remove it from the perturbation calculation. Even more importantly, using this new generalized order concept, CP series can be determined for molecular properties of ground and excited states and for transition properties between these states, including excitation energies and energies of the excited states. The applicability of CP theory to both the energy and molecular properties and numerical results for the CP energy and molecular property series demonstrate the superiority of CP theory compared to previous perturbation models. Low-order corrections in the CP perturbation series can be expected soon to become state-of-the-art electronic structure models for the determination of energies and molecular properties of target-state quality for single-configuration dominated molecular systems.

I. INTRODUCTION

Møller-Plesset perturbation theory (MPPT) is a standard wave-function method for determining ground-state energies[1,2] and static ground-state molecular properties.[3–6] The zeroth-order state in MPPT is the Hartree-Fock (HF) state, and the target energy and the target molecular properties are the ones of full configuration-interaction (FCI) wave function calculations. The major drawbacks of MPPT are the following:

1. The zeroth-order state is a non-correlated HF state.
2. The target energy and static molecular properties are the ones of FCI calculations. High excitation levels are therefore considered even if these only have little or no effect on the calculated energy and molecular properties.
3. MPPT can be applied only to the ground-state energy and static molecular properties.
4. The zeroth-order energy and static molecular properties are determined by the Fock operator, and the perturbation corrections, required to obtain the FCI energy and static molecular properties, therefore become large. The zeroth-order ground-state energy is thus a sum of the orbital energies for the occupied orbitals of the HF state, and the target energy is the FCI energy. Hence, the energy correction in MPPT is large and, in particular, much larger than the correlation energy.

5. The MPPT perturbation series for the ground-state energy and static molecular properties are plagued by divergences also for single-configuration dominated molecular systems, in particular when augmented basis sets are used that contain diffuse functions.[7,8]

In this paper, we introduce a new class of perturbation models—the cluster perturbation (CP) models—where the major drawbacks of MPPT have been overcome. We describe below the general features of CP theory and how the major drawbacks of MPPT are removed. MPPT has recently been generalized to coupled cluster perturbation theory (CCPT).[9–11] We also discuss the relation between CP theory and CCPT and the advantages of using CP theory compared to CCPT.

In CP theory, we consider a target excitation space relative to an HF state and partition the target excitation space into a parent excitation space and an auxiliary excitation space. The zeroth-order state in CP theory is a coupled cluster (CC) state in the parent excitation space. In CP theory, we thus use a correlated zeroth-order state and not a non-correlated HF state as in MPPT.

In CP theory, we consider target states that are expanded either in terms of the many-body excitation operators or the state-transfer operators of the target excitation space. Furthermore, the target states are expanded with the CC parent state as an expansion point. Using the many-body excitation operators, the CP target states become exponentially parameterized and describe standard CC states but in a non-conventional parameterization. Using state-transfer operators, the CP target state becomes linearly parameterized and will be denoted as the cluster linear (CL) target state. CP target states can be truncated at an arbitrary excitation level, and therefore high excitation levels, which have little or no effect on the energy or molecular property, do not need to be considered. We assume in this paper that the CP target state is a CC state and defer the derivation of CP theory for CL target states to Paper V of this series.[12]

In CP theory, we determine perturbation series in orders of the perturbation operator that in CP theory is the CC parent-state similarity-transformed fluctuation potential. We determine CP series for both the energy and molecular properties, including excitation energies. The zeroth-order term in the CP series is the energy or molecular property of the CP parent state, and the CP series formally converge to the energy or molecular property of the CP target state. The perturbation corrections that are determined in CP theory both for the energy and for molecular properties are small and consist of the difference between the energy and molecular property for the CC parent and the CC target state.

The requirement that the CP target state is expanded with the CC parent state as the expansion point defines a unique pathway connecting the determination of the CC parent state and the CC target state and is one of the important features that make it possible to determine CP series for both the energy and molecular properties. Molecular properties are in CP theory determined using response function theory, where the response functions for the CC parent state determine the molecular properties for the CC parent state and where the response functions for the CC target state determine the molecular properties for the CC target state.

To determine perturbation series for the energy and for molecular properties on an equal footing also requires that we introduce a new generalized order concept, where selected fluctuation potential contributions are treated as zeroth-order contributions. The CC parent-state Jacobian contains a fluctuation potential contribution, but it, nevertheless, is treated in CP theory as a zeroth-order term. In practice, this is done by solving sets of linear equations in the parent excitation space that contains the CC parent-state Jacobian when cluster amplitudes and response amplitudes are determined. By treating the CC parent-state Jacobian as a zeroth-order contribution, internal relaxation in the parent excitation space is treated at zeroth order, and hence it is removed from the energy and response function perturbation calculations.

MPPT has been generalized to coupled cluster perturbation theory (CCPT), where the zeroth-order state, as in CP theory, is a CC state in the parent excitation space and where the target state is a CC state.[9–11] Using CCPT, two energy series similar to the energy series of CP theory have been developed.[9,11] The main difference between these two series is that for the series of Kristensen *et al.*,[11] the energy of the CC target state is parameterized with the CC parent state as the expansion point, while for the series of Eriksen *et al.*,[9] the energy Lagrangian is parameterized with the CC parent state and its bi-orthonormal parent multiplier state as the expansion point. The energy Lagrangian thus contains information about both the CC target state and its bi-orthonormal multiplier state, which stabilizes the convergence of the Lagrangian series compared to the energy series.[11] We denote the CCPT series of Kristensen *et al.*[11] as the CCPT energy series and the series of Eriksen *et al.*[9] as the CCPT Lagrangian series. The CCPT energy series may be obtained from the CP series if the CC parent state Jacobian is divided into a Fock operator contribution and a fluctuation potential contribution, and terms are collected strictly as zeroth-order Fock operator contributions and first-order fluctuation potential contributions. Collecting terms strictly as zeroth-order Fock operator contributions and first-order fluctuation potential contributions, when solving amplitude equations, is common to both the CCPT energy and the CCPT Lagrangian method and stands in contrast to CP theory, where one fluctuation potential contribution—the fluctuation potential contribution in the parent-state Jacobian—is treated as a zeroth-order contribution. CCPT can be used to determine ground-state energy series but not molecular property series.

For MPPT, it has been shown that divergence of the perturbation energy series is the rule rather than exception for basis sets containing diffuse functions.[7,8,13] For the CCPT energy series, it has also been shown that the underlying conditions for convergence (divergence) of the CCPT series are the same as for the MPPT series.[14] The requirements for convergence of CP energy series differ from the ones of the MPPT and CCPT series. The theoretical foundation for convergent CP energy series is described in Paper IV,[15] where it is also shown how the asymptotic convergence of the CP energy series can be modeled using a simple two-state model. The asymptotic convergence of the CP energy series determines the convergence rate and the convergence patterns of the higher-order terms in the CP series.

In this paper, the theoretical foundation for determining CP series for the ground-state energy is developed for general parent and target excitation spaces. We also show that CP series can be determined for molecular properties, but the detailed derivation of CP molecular property series is deferred to future articles. Explicit

expressions are given for the lowest-order energy corrections for CP series with a CCSD parent state and a CCSDT target state, and the CP energy series are compared to the corresponding CCPT energy and CCPT Lagrangian series. We also report calculations for CP energy series for various parent and target excitation spaces and examine the convergence of these series. For the lower-order convergence, we examine how well these corrections can reproduce the total energy correction. The convergence rate and the convergence patterns of the higher-order terms in the CP energy series are also examined using the two-state model. To carry out this examination, we rely on the thorough analysis of the two-state model that has been performed in Ref. 16. Finally, the performance of the CP energy series is compared with the one of the CCPT energy and CCPT Lagrangian series.

An extensive literature exists for the determination of an energy correction to a CC parent-state energy arising from an excitation level that is higher than that of the parent state. This literature has been reviewed in Ref. 9 and presented from the perspective of CCPT. As CP series for the ground-state energy describe an extension of the CCPT series, we refer to Ref. 9 for a review of the literature, where also a CP perspective can partly be obtained. To exemplify this perspective, we consider a CP energy series for the CCSD parent state, where the energy corrections converge to the CCSDT energy. The CP series has non-vanishing contributions that start in third order. The third- and fourth-order corrections contain triples contributions, which are identical to the two lowest non-vanishing order contributions in the CCPT Lagrangian series and to the two lowest non-vanishing order triples-only contributions in the CC(2)PT(m) series of Hirata *et al.*[17–19] Furthermore, the triples-only contribution in the CCSD(2) model of Gwaltney and Head-Gordon[20,21] gives the third-order contribution in the CP series, whereas in the method of moments of CC (MMCC) equations of Piecuch and co-workers,[22–24] the third-order contribution in the CP series is also obtained but with the denominators in the energy corrections being those of Epstein-Nesbet second-order perturbation theory rather than the orbital-energy differences of Møller-Plesset perturbation theory. Both the CCPT Lagrangian series and the CP energy series are developed within a CC framework, and they may therefore target the CCSDT energy, whereas the other methods are developed within an EOM-CC framework[25,26] and therefore have to target the FCI energy. In the fifth order, the CP series contains relaxation contributions in the singles-and-doubles sub-space due to the presence of the triples excitation space, and the energy contributions of the CCPT Lagrangian series and of the CP series start to differ at this order as they also do in higher orders. For the methods developed within the EOM-CC framework, it has turned out to be difficult to obtain a proper description of the higher-order contributions, where, for example, the energy corrections are size-extensive.

In Sec. II, the theoretical framework for CP theory is established and CP energy series are derived for arbitrary parent and target excitation spaces. We further show that CP series can also be derived for molecular properties. In Sec. III, the lowest-order energy corrections are determined through fifth order for the CP energy series with a CCSD parent state and a CCSDT target state, and the CP energy corrections are compared with the ones of the CCPT Lagrangian series. The mathematical theory needed for analyzing the convergence of perturbation theory is summarized in Sec. IV, where we also review the two-state model and the convergence archetypes that can be encountered for perturbation series, which effectively become a two-state problem at higher orders. In Sec. V, we present calculations of CP energy series for general CC parent and CC target states. Section VI contains a short summary and concluding remarks.

II. THEORETICAL FRAMEWORK FOR CLUSTER PERTURBATION (CP) THEORY

A. Standard coupled cluster theory

In CC theory,[8,27] the wave function is exponentially parameterized,

$$|\mathrm{CC}\rangle = \mathrm{e}^{T}|\mathrm{HF}\rangle, \tag{1}$$

where the cluster operator,

$$T = \sum_{\mu_i} t_{\mu_i}\theta_{\mu_i}, \tag{2}$$

contains the cluster amplitudes t_{μ_i} and the many-body excitation operators θ_{μ_i} that acting on the Hartree-Fock state $|\mathrm{HF}\rangle$ produce its orthogonal complement set of states,

$$|\mu_i\rangle = \theta_{\mu_i}|\mathrm{HF}\rangle. \tag{3}$$

In Eqs. (2) and (3), i denotes an excitation level and μ_i an excitation at this level.

The CC Schrödinger equation may be expressed as

$$\mathrm{e}^{-T}H_0\mathrm{e}^{T}|\mathrm{HF}\rangle = E_0|\mathrm{HF}\rangle, \tag{4}$$

where H_0 is the Hamiltonian and E_0 is the ground-state energy. The CC Schrödinger equation may be solved by projection against the basis $\langle\mathcal{B}| = |\mathcal{B}\rangle^{\dagger}$, where

$$|\mathcal{B}\rangle = \Big\{|\mathrm{HF}\rangle, |\mu_i\rangle, \qquad i = 1, 2, \ldots\Big\}, \tag{5}$$

leading to the CC energy and amplitude equations,

$$E_0 = \langle\mathrm{HF}|\mathrm{e}^{-T}H_0\mathrm{e}^{T}|\mathrm{HF}\rangle = \langle\mathrm{HF}|H_0|\mathrm{HF}\rangle + \langle\mathrm{HF}|H_0T_2|\mathrm{HF}\rangle + \frac{1}{2}\langle\mathrm{HF}|H_0T_1^2|\mathrm{HF}\rangle, \tag{6}$$

$$\langle\mu_i|\mathrm{e}^{-T}H_0\mathrm{e}^{T}|\mathrm{HF}\rangle = 0, \tag{7}$$

where we have used the Brillouin theorem to obtain the energy in Eq. (6). In a standard coupled cluster calculation, a CC state with a truncated cluster operator is determined in a truncated excitation space, which we denote as the *target excitation space*. The cluster amplitudes are determined from the cluster amplitude equations in Eq. (7) in the target excitation space, and the energy is determined from Eq. (6). In this paper, we introduce *cluster perturbation* (CP) theory where the amplitudes and the energy of the CC target state are determined using perturbation theory.

B. Amplitude equations in CP theory

In CP theory, we consider a target excitation space ($1 \le i \le t$) that is partitioned into a *parent excitation space* ($1 \le i \le p$) and an *auxiliary excitation space* ($p < i \le t$). The zeroth-order state is a CC state in the parent excitation space,

$$|\mathrm{CC}^*\rangle = \mathrm{e}^{{}^*T}|\mathrm{HF}\rangle, \tag{8}$$

where the cluster amplitudes satisfy the cluster amplitude equation in the parent excitation space,

$$\langle\mu_i|\mathrm{e}^{-{}^*T}H_0\mathrm{e}^{{}^*T}|\mathrm{HF}\rangle = 0, \qquad 1 \le i \le p, \tag{9}$$

$${}^*T = {}^*T_1 + \cdots + {}^*T_p, \tag{10}$$

$${}^*T_i = \sum_{\mu_i} {}^*t_{\mu_i}\theta_{\mu_i}, \qquad 1 \le i \le p, \tag{11}$$

and where the parent-state energy is

$${}^*E_0 = \langle\mathrm{HF}|\mathrm{e}^{-{}^*T}H_0\mathrm{e}^{{}^*T}|\mathrm{HF}\rangle. \tag{12}$$

In this paper, the target state is assumed to be a CC target state that is parameterized in terms of the CC parent state embedded in an exponentially parameterized target excitation space,

$$|\mathrm{CC}\rangle = \mathrm{e}^{T}|\mathrm{HF}\rangle = \mathrm{e}^{\delta T + {}^*T}|\mathrm{HF}\rangle = \mathrm{e}^{\delta T}|\mathrm{CC}^*\rangle, \tag{13}$$

where

$$\delta T = \sum_{i=1}^{t}\sum_{\mu_i}\delta t_{\mu_i}\theta_{\mu_i}. \tag{14}$$

CP theory can also be developed for target states where the embedding of the CC parent state in the target excitation space is described using a linear parameterization. We refer to such CP target states as cluster linear (CL) target states. The development of CP theory for CL target states is addressed in Paper V.[12]

The similarity-transformed Schrödinger equation for the CP target state in Eq. (13) may be written as

$$\mathrm{e}^{-\delta T}\mathrm{e}^{-{}^*T}H_0\mathrm{e}^{{}^*T}\mathrm{e}^{\delta T}|\mathrm{HF}\rangle = E_0|\mathrm{HF}\rangle. \tag{15}$$

Projecting Eq. (15) against the basis $\langle\mathcal{B}| = |\mathcal{B}\rangle^\dagger$ of Eq. (5) gives the energy and amplitude equations,

$$E_0 = \langle\mathrm{HF}|\mathrm{e}^{-\delta T}\mathrm{e}^{-{}^*T}H_0\mathrm{e}^{{}^*T}\mathrm{e}^{\delta T}|\mathrm{HF}\rangle = \langle\mathrm{HF}|\mathrm{e}^{-\delta T}H_0^{*T}\mathrm{e}^{\delta T}|\mathrm{HF}\rangle, \tag{16}$$

$$\langle\mu_i|\mathrm{e}^{-\delta T}\mathrm{e}^{-{}^*T}H_0\mathrm{e}^{{}^*T}\mathrm{e}^{\delta T}|\mathrm{HF}\rangle = \langle\mu_i|\mathrm{e}^{-\delta T}H_0^{*T}\mathrm{e}^{\delta T}|\mathrm{HF}\rangle = 0, \ 1 \le i \le t, \tag{17}$$

with

$$H_0^{*T} = \mathrm{e}^{-{}^*T}H_0\mathrm{e}^{{}^*T}. \tag{18}$$

To determine the amplitude corrections, δt_{μ_i}, we carry out a Baker-Campbell-Hausdorff (BCH) expansion in the amplitude equations of Eq. (17),

$$\begin{aligned}&\langle\mu_i|H_0^{*T}|\mathrm{HF}\rangle S_{ip} + \sum_{j=1}^{t}\sum_{\nu_j}\langle\mu_i|\big[H_0^{*T},\theta_{\nu_j}\big]|\mathrm{HF}\rangle\delta t_{\nu_j}\\ &+\frac{1}{2}\langle\mu_i|\big[\big[H_0^{*T},\delta T\big],\delta T\big]|\mathrm{HF}\rangle + \frac{1}{6}\langle\mu_i|\big[\big[\big[H_0^{*T},\delta T\big],\delta T\big],\delta T\big]|\mathrm{HF}\rangle\\ &+\frac{1}{24}\langle\mu_i|\big[\big[\big[\big[H_0^{*T},\delta T\big],\delta T\big],\delta T\big],\delta T\big]|\mathrm{HF}\rangle = 0, \quad 1 \le i \le t; \quad p < t,\end{aligned} \tag{19}$$

where to obtain the first term, we have used Eq. (9) and introduced the integer step function S_{ab},

$$S_{ab} = \begin{cases}0, & \text{for } a \le b\\ 1, & \text{for } a > b.\end{cases} \tag{20}$$

Introducing the Møller-Plesset partitioning of the Hamiltonian,

$$H_0 = f + \Phi, \tag{21}$$

where f is the Fock operator in the canonical Hartree-Fock basis and Φ is the fluctuation potential, we determine in CP theory amplitude corrections to the CC parent state in orders of the CC parent state similarity-transformed fluctuation potential and write the amplitude equations [Eq. (19)] as

$$\begin{aligned}&\langle\mu_i|\Phi^{*T}|\mathrm{HF}\rangle S_{ip} + \sum_{j=1}^{t}\sum_{\nu_j}\langle\mu_i|\big[H_0^{*T},\theta_{\nu_j}\big]|\mathrm{HF}\rangle\delta t_{\nu_j}\\ &+\frac{1}{2}\langle\mu_i|\big[\big[\Phi^{*T},\delta T\big],\delta T\big]|\mathrm{HF}\rangle + \frac{1}{6}\langle\mu_i|\big[\big[\big[\Phi^{*T},\delta T\big],\delta T\big],\delta T\big]|\mathrm{HF}\rangle\\ &+\frac{1}{24}\langle\mu_i|\big[\big[\big[\big[\Phi^{*T},\delta T\big],\delta T\big],\delta T\big],\delta T\big]|\mathrm{HF}\rangle = 0, \quad 1 \le i \le t; \quad p < t,\end{aligned} \tag{22}$$

where we have used

$$\begin{aligned}\langle\mu_i|[f,{}^*T]|\mathrm{HF}\rangle S_{ip} &= \sum_{j=1}^{p}\sum_{\nu_j}{}^*t_{\nu_j}\langle\mu_i|\big[f,\theta_{\nu_j}\big]|\mathrm{HF}\rangle S_{ip}\\ &= \sum_{j=1}^{p}\sum_{\nu_j}\varepsilon_{\nu_j}{}^*t_{\nu_j}\langle\mu_i|\theta_{\nu_j}|\mathrm{HF}\rangle S_{ip} = 0, \ 1 \le i \le t; \ p < t.\end{aligned} \tag{23}$$

To obtain the second equality in Eq. (23), we have used the commutator relation

$$[f,\theta_{\mu_i}] = \varepsilon_{\mu_i}\theta_{\mu_i}, \tag{24}$$

where

$$\varepsilon_{\mu_i} = \langle\mu_i|f|\mu_i\rangle - \langle\mathrm{HF}|f|\mathrm{HF}\rangle \tag{25}$$

denotes orbital energy differences between orbitals that are occupied in the state $|\mu_i\rangle = \theta_{\mu_i}|\mathrm{HF}\rangle$ and in the Hartree-Fock state $|\mathrm{HF}\rangle$. To obtain the last equality in Eq. (23), we have used that the excitation levels i and j belong to different excitation spaces since $i > p$ and $j \le p$. Furthermore, to obtain Eq. (22), we have used that the Fock operator contribution vanishes for all terms involving two or more commutators.

The target-state amplitude equations in Eq. (22) may be written as

$$\begin{aligned}\sum_{j=1}^{t}\sum_{\nu_j}A_{\mu_i\nu_j}\delta t_{\nu_j} = &-\langle\mu_i|\Phi^{*T}|\mathrm{HF}\rangle S_{ip} - \frac{1}{2}\langle\mu_i|\big[\big[\Phi^{*T},\delta T\big],\delta T\big]|\mathrm{HF}\rangle\\ &-\frac{1}{6}\langle\mu_i|\big[\big[\big[\Phi^{*T},\delta T\big],\delta T\big],\delta T\big]|\mathrm{HF}\rangle\\ &-\frac{1}{24}\langle\mu_i|\big[\big[\big[\big[\Phi^{*T},\delta T\big],\delta T\big],\delta T\big],\delta T\big]|\mathrm{HF}\rangle,\\ &1 \le i \le t; \quad p < t,\end{aligned} \tag{26}$$

where we have introduced the extended CC parent-state Jacobian

$$A_{\mu_i\nu_j} = \frac{\mathrm{d}}{\mathrm{d}\delta t_{\nu_j}} \langle \mu_i | \mathrm{e}^{-\delta T} H_0^{*T} \mathrm{e}^{\delta T} | \mathrm{HF} \rangle \Big|_{\delta t=0}$$
$$= \langle \mu_i | \big[H_0^{*T}, \theta_{\nu_j} \big] | \mathrm{HF} \rangle = \varepsilon_{\nu_j} \delta_{\mu_i\nu_j} + \langle \mu_i | \big[\Phi^{*T}, \theta_{\nu_j} \big] | \mathrm{HF} \rangle, \quad 1 \le i,j \le t. \tag{27}$$

To obtain the last equality in Eq. (27), we have used that

$$\langle \mu_i | \big[f^{*T}, \theta_{\nu_j} \big] | \mathrm{HF} \rangle = \varepsilon_{\nu_j} \delta_{\mu_i\nu_j}, \qquad 1 \le i,j \le t. \tag{28}$$

The amplitudes of the CC target state can be determined solving Eq. (26) using perturbation theory with Φ^{*T} as the perturbation operator. This can be done by partitioning the extended CC parent-state Jacobian into a zeroth- and a first-order component,

$$A_{\mu_i\nu_j} = A^{(0)}_{\mu_i\nu_j} + A^{(1)}_{\mu_i\nu_j}. \tag{29}$$

Substituting Eq. (29) in Eq. (26) gives the amplitude equation

$$\sum_{j=1}^{t} \sum_{\nu_j} A^{(0)}_{\mu_i\nu_j} \delta t_{\nu_j} = -\langle \mu_i | \Phi^{*T} | \mathrm{HF} \rangle S_{ip} - \sum_{j=1}^{t} \sum_{\nu_j} A^{(1)}_{\mu_i\nu_j} \delta t_{\nu_j}$$
$$- \frac{1}{2} \langle \mu_i | \big[\big[\Phi^{*T}, \delta T \big], \delta T \big] | \mathrm{HF} \rangle$$
$$- \frac{1}{6} \langle \mu_i | \big[\big[\big[\Phi^{*T}, \delta T \big], \delta T \big], \delta T \big] | \mathrm{HF} \rangle$$
$$- \frac{1}{24} \langle \mu_i | \big[\big[\big[\big[\Phi^{*T}, \delta T \big], \delta T \big], \delta T \big], \delta T \big] | \mathrm{HF} \rangle,$$
$$1 \le i \le t; \quad p < t. \tag{30}$$

Solving Eq. (30) order by order in Φ^{*T} requires that the extended parent-state Jacobian $\mathbf{A}$ is partitioned explicitly into a zeroth- and first-order component, where $\mathbf{A}^{(1)}$ may only contain contributions that are linear in Φ^{*T} and $\mathbf{A}^{(0)}$ has to contain all the zeroth-order Fock operator terms. However, $\mathbf{A}^{(0)}$ can also contain one or several of the fluctuation potential terms of $\mathbf{A}$. Whenever $\mathbf{A}^{(0)}$ contains fluctuation potential terms, these terms are treated as zeroth-order contributions and we have in this way generalized the order concept of standard perturbation theory. This is of particular interest when $\mathbf{A}^{(0)}$ can be inverted without affecting the leading-order computational scaling characteristic for determining the cluster amplitudes from the cluster amplitude equations in Eq. (30).

The fastest-convergent perturbation series is obtained by choosing $\mathbf{A}^{(0)}$ as the full extended CC parent-state Jacobian, $\mathbf{A}$, with a vanishing $\mathbf{A}^{(1)}$ contribution. This series will describe a fixed Hessian series and is linearly convergent. However, the computational scaling makes this series non-tractable as this partitioning requires that sets of linear equations containing the full extended CC parent-state Jacobian in Eq. (27) are solved in the target excitation space at each order to obtain the cluster amplitude corrections.

In CCPT, the amplitude equations are obtained by assigning all Fock operator contributions of $\mathbf{A}$ to $\mathbf{A}^{(0)}$ and all fluctuation potential terms to $\mathbf{A}^{(1)}$. In Subsection II C, we describe how the amplitude equations are solved in CCPT. We further discuss how internal relaxation in the parent sub-space is partly removed from perturbation calculation in CCPT by parameterizing the target-state cluster amplitudes, $t = {}^*t + \delta t$, with the parent-state cluster amplitudes, ${}^*t$ of Eq. (11), as the expansion point [see Eq. (13)]. However, we also describe that the amplitude corrections in CCPT still contain internal relaxation contributions in the parent excitation space. In Subsection II D, we introduce CP theory, in which internal relaxation in the parent sub-space is *fully* removed from the perturbation calculation. This is a key feature of CP theory, which allows for two fundamental improvements compared to CCPT: First, as the internal relaxation in the parent excitation space can be large, its removal from the perturbation calculation can lead to a faster-convergent energy series. Second, and particularly important, this removal makes it possible to determine CP series on an equal footing for the energy and for molecular properties, including frequency-dependent properties, transition properties, and excitation energies.

C. CCPT amplitude equations

When the amplitude equations in Eq. (30) are solved in CCPT theory, the extended CC parent-state Jacobian is partitioned into a zeroth-order component, $\mathbf{A}^{(0)}$, that contains the Fock operator terms and a first-order component, $\mathbf{A}^{(1)}$, that contains the Φ^{*T} terms,

$$A^{(0)}_{\mu_i\nu_j} = \varepsilon_{\nu_j} \delta_{\mu_i\nu_j}, \qquad 1 \le i,j \le t, \tag{31a}$$
$$A^{(1)}_{\mu_i\nu_j} = \langle \mu_i | \big[\Phi^{*T}, \theta_{\nu_j} \big] | \mathrm{HF} \rangle, \qquad 1 \le i,j \le t. \tag{31b}$$

We denote this partitioning of $\mathbf{A}$ as the *Fock operator partitioning*. Substituting Eq. (31) into Eq. (30) gives

$$\varepsilon_{\mu_i} \delta t_{\mu_i} = -\langle \mu_i | \Phi^{*T} | \mathrm{HF} \rangle S_{ip} - \sum_{j=1}^{t} \sum_{\nu_j} \langle \mu_i | \big[\Phi^{*T}, \theta_{\nu_j} \big] | \mathrm{HF} \rangle \delta t_{\nu_j}$$
$$- \frac{1}{2} \langle \mu_i | \big[\big[\Phi^{*T}, \delta T \big], \delta T \big] | \mathrm{HF} \rangle$$
$$- \frac{1}{6} \langle \mu_i | \big[\big[\big[\Phi^{*T}, \delta T \big], \delta T \big], \delta T \big] | \mathrm{HF} \rangle$$
$$- \frac{1}{24} \langle \mu_i | \big[\big[\big[\big[\Phi^{*T}, \delta T \big], \delta T \big], \delta T \big], \delta T \big] | \mathrm{HF} \rangle, \quad 1 \le i \le t. \tag{32}$$

Equation (32) may be solved order by order in Φ^{*T} giving the kth order amplitude equations

$$\varepsilon_{\mu_i} \delta t^{(k)}_{\mu_i} = -\langle \mu_i | \Phi^{*T} | \mathrm{HF} \rangle S_{ip} \delta_{k1} - \sum_{j=1}^{t} \sum_{\nu_j} \langle \mu_i | \big[\Phi^{*T}, \theta_{\nu_j} \big] | \mathrm{HF} \rangle \delta t^{(k-1)}_{\nu_j}$$
$$- \Bigg\{ \frac{1}{2} \langle \mu_i | \big[\big[\Phi^{*T}, \delta T \big], \delta T \big] | \mathrm{HF} \rangle$$
$$+ \frac{1}{6} \langle \mu_i | \big[\big[\big[\Phi^{*T}, \delta T \big], \delta T \big], \delta T \big] | \mathrm{HF} \rangle$$
$$- \frac{1}{24} \langle \mu_i | \big[\big[\big[\big[\Phi^{*T}, \delta T \big], \delta T \big], \delta T \big], \delta T \big] | \mathrm{HF} \rangle \Bigg\}^{\{k\}}, \quad 1 \le i \le t, \tag{33}$$

where $\{ \, . \, \}^{\{k\}}$ denotes that the terms of order k in Φ^{*T} are picked up and gathered from the expression in the parentheses. The amplitude corrections of Eq. (33), when inserted in Eq. (16), give the CCPT energy series of Kristensen *et al.*[11]

Internal relaxation in the parent excitation space is described by the ${}^*\mathbf{t}$ amplitudes, which satisfy the cluster amplitude equations in the parent excitation space in Eq. (9). When deriving the CCPT

cluster amplitude equations in Eq. (32), the first term on the right-hand side is obtained using Eq. (9). In CCPT, internal relaxation in the parent excitation space is therefore partly removed by using the parent-state cluster amplitudes $^*\mathbf{t}$ as the expansion point for the CC target-state amplitudes. Note that by using $^*\mathbf{t}$ as the expansion point, it is Φ^{*T}, rather than Φ, that becomes the perturbation operator. However, the CCPT amplitudes determined from Eq. (32) still contain a contribution [the second term on the right-hand side of Eq. (32)]

$$\sum_{j=1}^{p}\sum_{\nu_j}\langle\mu_i|\big[\Phi^{*T},\theta_{\nu_j}\big]|\mathrm{HF}\rangle\delta t_{\nu_j}, \qquad 1\le i\le p$$

that describes internal relaxation in the parent excitation space. To fully remove internal relaxation in the parent excitation space from the perturbation calculation, we have to move this term to the left-hand side in Eq. (32) and treat it as a zeroth-order contribution. This is what is done in CP theory, as we will describe in Subsection II D.

D. CP amplitude equations

We will now describe how the cluster amplitude equations can be derived in CP theory. As discussed in Subsection II C, the CP cluster amplitude equations are obtained by moving the internal relaxation contribution in the second term on the right-hand side of Eq. (32) to the left-hand side of this equation, giving

$$\begin{aligned}
&\sum_{j=1}^{t}\sum_{\nu_j}\Big(\varepsilon_{\mu_i}\delta_{\mu_i\nu_j}+\langle\mu_i|\big[\Phi^{*T},\theta_{\nu_j}\big]|\mathrm{HF}\rangle(1-S_{ip})(1-S_{jp})\Big)\delta t_{\nu_j}\\
&\quad=-\langle\mu_i|\Phi^{*T}|\mathrm{HF}\rangle S_{ip}-\sum_{j=p+1}^{t}\sum_{\nu_j}\langle\mu_i|\big[\Phi^{*T},\theta_{\nu_j}\big]|\mathrm{HF}\rangle\delta t_{\nu_j}\\
&\qquad-\sum_{j=1}^{p}\sum_{\nu_j}\langle\mu_i|\big[\Phi^{*T},\theta_{\nu_j}\big]|\mathrm{HF}\rangle\delta t_{\nu_j}S_{ip}-\frac{1}{2}\langle\mu_i|\big[\big[\Phi^{*T},\delta T\big],\delta T\big]|\mathrm{HF}\rangle\\
&\qquad-\frac{1}{6}\langle\mu_i|\big[\big[\big[\Phi^{*T},\delta T\big],\delta T\big],\delta T\big]|\mathrm{HF}\rangle\\
&\qquad-\frac{1}{24}\langle\mu_i|\big[\big[\big[\big[\Phi^{*T},\delta T\big],\delta T\big],\delta T\big],\delta T\big]|\mathrm{HF}\rangle, \qquad 1\le i\le t. \quad (34)
\end{aligned}$$

Equation (34) can conveniently be partitioned into a parent- and an auxiliary-space component as

$$\begin{aligned}
&\sum_{j=1}^{p}\sum_{\nu_j}J^{P}_{\mu_i\nu_j}\delta t^{(k)}_{\nu_j}\\
&\quad=-\sum_{j=p+1}^{t}\sum_{\nu_j}\langle\mu_i|\big[\Phi^{*T},\theta_{\nu_j}\big]|\mathrm{HF}\rangle\delta t^{(k-1)}_{\nu_j}\\
&\qquad-\Big(\frac{1}{2}\langle\mu_i|\big[\big[\Phi^{*T},\delta T\big],\delta T\big]|\mathrm{HF}\rangle\\
&\qquad+\frac{1}{6}\langle\mu_i|\big[\big[\big[\Phi^{*T},\delta T\big],\delta T\big],\delta T\big]|\mathrm{HF}\rangle\\
&\qquad+\frac{1}{24}\langle\mu_i|\big[\big[\big[\big[\Phi^{*T},\delta T\big],\delta T\big],\delta T\big],\delta T\big]|\mathrm{HF}\rangle\Big)^{(k)}, \qquad 1\le i\le p,
\end{aligned} \quad (35a)$$

$$\begin{aligned}
\varepsilon_{\mu_i}\delta t^{(k)}_{\mu_i}&=-\langle\mu_i|\Phi^{*T}|\mathrm{HF}\rangle\delta_{k1}-\sum_{j=1}^{t}\sum_{\nu_j}\langle\mu_i|\big[\Phi^{*T},\theta_{\nu_j}\big]|\mathrm{HF}\rangle\delta t^{(k-1)}_{\nu_j}\\
&\quad-\Big(\frac{1}{2}\langle\mu_i|\big[\big[\Phi^{*T},\delta T\big],\delta T\big]|\mathrm{HF}\rangle\\
&\quad+\frac{1}{6}\langle\mu_i|\big[\big[\big[\Phi^{*T},\delta T\big],\delta T\big],\delta T\big]|\mathrm{HF}\rangle\\
&\quad+\frac{1}{24}\langle\mu_i|\big[\big[\big[\big[\Phi^{*T},\delta T\big],\delta T\big],\delta T\big],\delta T\big]|\mathrm{HF}\rangle\Big)^{(k)}, \qquad p<i\le t,
\end{aligned} \quad (35b)$$

where we have introduced the CC parent-state Jacobian,

$$\begin{aligned}
J^{P}_{\mu_i\nu_j}&=\langle\mu_i|\big[H_0^{*T},\theta_{\nu_j}\big]|\mathrm{HF}\rangle(1-S_{ip})(1-S_{jp})\\
&=\Big(\langle\mu_i|H_0^{*T}|\nu_j\rangle-\langle\mathrm{HF}|H_0^{*T}|\mathrm{HF}\rangle\delta_{\mu_i\nu_j}\Big)\\
&\quad\times(1-S_{ip})(1-S_{jp}), \qquad 1\le i,j\le t.
\end{aligned} \quad (36)$$

When the kth-order amplitude corrections are determined in CP theory, sets of linear equations containing the parent-state Jacobian have to be solved in the parent excitation space. Equation (35a) substantiates that internal relaxation in the parent excitation space is removed from the perturbation calculation since the first term on the right-hand side of Eq. (35a) only introduces a coupling between the parent excitation space and the auxiliary excitation space.

The amplitude corrections in Eqs. (35) determine the CP energy series. The two lowest-order amplitude corrections read

$$\delta t^{(1)}_{\mu_i}=0, \qquad 1\le i\le p, \quad (37a)$$

$$\varepsilon_{\mu_i}\delta t^{(1)}_{\mu_i}=-\langle\mu_i|\Phi^{*T}|\mathrm{HF}\rangle, \qquad p<i\le t, \quad (37b)$$

$$\sum_{j=1}^{p}\sum_{\nu_j}J^{P}_{\mu_i\nu_j}\delta t^{(2)}_{\nu_j}=-\sum_{j=p+1}^{t}\sum_{\nu_j}\langle\mu_i|\big[\Phi^{*T},\theta_{\nu_j}\big]|\mathrm{HF}\rangle\delta t^{(1)}_{\nu_j}, \qquad 1\le i\le p, \quad (38a)$$

$$\varepsilon_{\mu_i}\delta t^{(2)}_{\mu_i}=-\sum_{j=p+1}^{t}\sum_{\nu_j}\langle\mu_i|\big[\Phi^{*T},\theta_{\nu_j}\big]|\mathrm{HF}\rangle\delta t^{(1)}_{\nu_j}, \qquad p<i\le t. \quad (38b)$$

Equation (34) shows that the extended CC parent-state Jacobian of CP theory in Eq. (29) is partitioned as

$$\begin{aligned}
A^{(0)}_{\mu_i\nu_j}&=\langle\mu_i|\big[H_0^{*T},\theta_{\nu_j}\big]|\mathrm{HF}\rangle(1-S_{ip})(1-S_{jp})\\
&\quad+\varepsilon_{\nu_j}\delta_{\mu_i\nu_j}S_{ip}S_{jp}, \qquad 1\le i,j\le t,
\end{aligned} \quad (39a)$$

$$\begin{aligned}
A^{(1)}_{\mu_i\nu_j}&=\langle\mu_i|\big[\Phi^{*T},\theta_{\nu_j}\big]|\mathrm{HF}\rangle(1-S_{ip})S_{jp}+\langle\mu_i|\big[\Phi^{*T},\theta_{\nu_j}\big]|\mathrm{HF}\rangle S_{ip}(1-S_{jp})\\
&\quad+\langle\mu_i|\big[\Phi^{*T},\theta_{\nu_j}\big]|\mathrm{HF}\rangle S_{ip}S_{jp}, \qquad 1\le i,j\le t.
\end{aligned} \quad (39b)$$

We denote this partitioning as the *parent-state Jacobian partitioning* of the extended CC parent-state Jacobian. An important feature of the parent-state Jacobian partitioning is that the parent-space sub-block of $\mathbf{A}^{(0)}$ contains the CC parent-state Jacobian $\mathbf{J}^P$ and thus a fluctuation potential contribution. The fluctuation potential contribution in the CC parent-state Jacobian is in CP theory treated as a zeroth-order contribution by solving sets of linear equations in the parent excitation sub-space [Eq. (35a)] containing $\mathbf{J}^P$. We have thus

introduced in CP theory a new generalized order concept, where one fluctuation potential contribution is treated as a zeroth-order contribution.

E. Equivalence between computational scaling of CP and CCPT

In CCPT, the Fock operator partitioning is used for the extended CC parent-state Jacobian, whereas in CP theory, the parent-state Jacobian partitioning is used. For both partitioning schemes, the right-hand sides of the auxiliary space amplitude equations contain the vector $\sum_{j=1}^{t}\sum_{v_j}\langle\mu_i|\big[\Phi^{*T},\theta_{v_j}\big]|\mathrm{HF}\rangle\delta t_{v_j}^{(k-1)}S_{ip}$, which introduces coupling between the parent and auxiliary excitation spaces and also a coupling internally in the auxiliary excitation space. In addition, for the Fock operator partitioning, the right-hand sides contain the vector

$$b_{\mu_i}^{(k)}(\delta t^{(k-1)}) = \sum_{j=1}^{p}\sum_{v_j}(1-S_{ip})\langle\mu_i|\big[\Phi^{*T},\theta_{v_j}\big]|\mathrm{HF}\rangle\delta t_{v_j}^{(k-1)}, \tag{40}$$

where coupling is introduced internally in the parent excitation space.

The main difference between the Fock operator partitioning and the parent-state Jacobian partitioning is that the fluctuation potential term of the CC parent-state Jacobian in Eq. (39a) is in the Fock operator partitioning a part of the perturbation and enters on the right-hand side of the amplitude equations. For the parent-state Jacobian partitioning, this fluctuation potential term of the CC parent-state Jacobian is treated as a zeroth-order contribution and it is therefore treated explicitly (*not* order-by-order) by solving sets of linear equations in the parent excitation space. In CP theory, we thus treat internal relaxation in the parent excitation space at zeroth order and hence remove it from the perturbation calculation. The parent-parent fluctuation potential block of the CC parent-state Jacobian can be large compared to the other fluctuation potential contributions, and a faster-convergent perturbation series is therefore obtained when the parent-state Jacobian partitioning is used, compared to the Fock operator partitioning.

The leading-order computational scaling is the same for the Fock operator partitioning and the parent-state Jacobian partitioning. To see this, recall that the right-hand sides of the two partitioning schemes differ by the term of Eq. (40) and that this term references only the parent space. The leading-order scaling for calculating this term therefore is N^{2p+2} where N refers to the size of the molecular system. By contrast, the calculation of, for example, the right-hand side terms $\sum_{j=p+1}^{t}\sum_{v_j}\langle\mu_i|\big[H_0^{*T},\theta_{v_j}\big]|\mathrm{HF}\rangle\delta t_{v_j}^{(k-1)}$ has a leading-order scaling that is at least N^{2p+4} and is thus at least two orders higher than the scaling for the term in Eq. (40). The leading-order scaling for constructing the right-hand sides in the two partitioning schemes is therefore equal. For the parent-state Jacobian partitioning, sets of linear equations [Eq. (35a)], which contain the parent state Jacobian of Eq. (36), also have to be solved. Solving these equations with iterative algorithms requires linear transformations that have the structure of Eq. (40), where Φ^{*T} is replaced by H_0^{*T}. As discussed above, these linear transformations do not affect the leading-order computational scaling and we can therefore conclude that the leading-order scaling is equal for the Fock operator and parent-state Jacobian partitioning schemes. We also note that the CC parent-state Jacobian partitioning of $\mathbf{A}$ used in CP theory is the only partitioning of $\mathbf{A}$, in which perturbation operator contributions can be moved to $\mathbf{A}^{(0)}$ yet retaining the leading-order computational scaling of the Fock operator partitioning.

F. Energy expansion in orders of the fluctuation potential

The ground-state energy may for both the Fock operator and the parent-state Jacobian partitioning be obtained from Eq. (16), giving

$$E_0 = {}^{*}E_0 + \sum_{k=2}^{\infty}E_0^{(k)}, \tag{41}$$

where ${}^{*}E_0$ is the parent-state energy of Eq. (12) and where the energy correction of order k is given by[11]

$$E_0^{(k)} = E_0^{(k)}(\mathrm{SD}) + E_0^{(k)}(\mathrm{SS}), \tag{42}$$

with

$$E_0^{(k)}(\mathrm{SD}) = \langle\mathrm{HF}|\big[\Phi^{*T},\delta T_1^{(k-1)}+\delta T_2^{(k-1)}\big]|\mathrm{HF}\rangle, \tag{43}$$

$$E_0^{(k)}(\mathrm{SS}) = \frac{1}{2}\sum_{h=2}^{k-3}\langle\mathrm{HF}|\big[\big[\Phi^{*T},\delta T_1^{(h)}\big],\delta T_1^{(k-h-1)}\big]|\mathrm{HF}\rangle. \tag{44}$$

G. CP theory for molecular properties

A CP energy series is defined by the perturbation operator, the parent and the target excitation space, the CC parent state, and the CC target state that identifies the target energy of the CP perturbation calculation. In addition, to fully define the CP perturbation series, we also have to specify that the parent-state Jacobian partitioning is used for the extended CC parent-state Jacobian. This last requirement is a new requirement that has to be implemented as all perturbation series have hitherto used the Fock operator partitioning in Eqs. (31). In this subsection, we show that using the parent-state Jacobian partitioning of the extended CC parent-state Jacobian, perturbation expansion may be determined also for molecular properties, where the CC parent-state molecular property becomes the zeroth-order term in the series and where the series formally converges to the molecular property of the CC target state.

For the CC target state, the energy and amplitude equations may be determined by projection using the bi-orthonormal basis

$$|\mathcal{B}^{*T}\rangle = \big\{\mathrm{e}^{*T}|\mathrm{HF}\rangle, \mathrm{e}^{*T}|\mu_i\rangle^{P}, \mathrm{e}^{*T}|\mu_i\rangle^{A}\big\}, \tag{45a}$$

$$\langle\mathcal{B}^{*T}| = \big\{\langle\mathrm{HF}|\mathrm{e}^{-*T}, {}^{P}\langle\mu_i|\mathrm{e}^{-*T}, {}^{A}\langle\mu_i|\mathrm{e}^{-*T}\big\}, \tag{45b}$$

where $|\mu_i\rangle^{P}$ and $|\mu_i\rangle^{A}$ denote the parent and auxiliary excitation space components, respectively, of the bi-orthonormal basis. Furthermore, for the parent-state Jacobian partitioning scheme, the zeroth-order component of the extended parent-state Jacobian may be written as

$$\boldsymbol{A}^{(0)} = \begin{pmatrix} {}^{P}\langle\mu_i|\mathrm{e}^{*T}\big[H_0,\theta_{v_j}\big]\mathrm{e}^{-*T}|\mathrm{HF}\rangle & \mathbf{0} \\ \mathbf{0} & {}^{A}\langle\mu_i|\mathrm{e}^{*T}\big[f,\theta_{v_j}\big]\mathrm{e}^{-*T}|\mathrm{HF}\rangle \end{pmatrix} = \begin{pmatrix} \mathbf{J}^{P} & \mathbf{0} \\ \mathbf{0} & \boldsymbol{\varepsilon}_{A} \end{pmatrix}, \tag{46}$$

where ε_A is a diagonal matrix containing orbital energy differences [see Eq. (28)] in the auxiliary space and $\mathbf{J}^P$ is the parent-state Jacobian of Eq. (36).

Consider now the parent-space subset of the bi-orthonormal basis in Eqs. (45),

$$|\mathcal{B}_P^{*T}\rangle = \left\{ e^{*T}|\mathrm{HF}\rangle, e^{*T}|\mu_i\rangle^P \right\}, \tag{47a}$$

$$\langle\mathcal{B}_P^{*T}| = \left\{ \langle \mathrm{HF}|e^{-{}^*T}, {}^P\langle\mu_i|e^{-{}^*T} \right\}. \tag{47b}$$

The Hamiltonian eigenvalue equation in this basis may be written as

$$\mathbf{H}_0^{*T}\,\mathbf{C}^{\mathrm{R}} = \mathbf{C}^{\mathrm{R}}\,{}^*\mathbf{E}, \tag{48a}$$

$$\mathbf{C}^{\mathrm{L}}\,\mathbf{H}_0^{*T} = {}^*\mathbf{E}\,\mathbf{C}^{\mathrm{L}}, \tag{48b}$$

$$\mathbf{C}^{\mathrm{L}}\,\mathbf{C}^{\mathrm{R}} = \mathbf{I}, \tag{48c}$$

where the Hamiltonian matrix has the block structure

$$\mathbf{H}_0^{*T} = \begin{pmatrix} {}^*E_0 & {}^P\boldsymbol{\eta} \\ \mathbf{0} & \left(\mathbf{H}_0^{*T}\right)^{\perp} \end{pmatrix}, \tag{49}$$

with

$$\left(\mathbf{H}_0^{*T}\right)_{\mathrm{HF\,HF}} = \langle \mathrm{HF}|e^{-{}^*T} H_0 e^{{}^*T}|\mathrm{HF}\rangle = {}^*E_0, \tag{50}$$

$$\left(\mathbf{H}_0^{*T}\right)_{\mu_i\,\mathrm{HF}} = {}^P\langle\mu_i|e^{-{}^*T} H_0 e^{{}^*T}|\mathrm{HF}\rangle = 0, \tag{51}$$

$$\left(\mathbf{H}_0^{*T}\right)_{\mathrm{HF}\,\mu_i} = \langle \mathrm{HF}|e^{-{}^*T} H_0 e^{{}^*T}|\mu_i\rangle^P = {}^P\eta_{\mu_i}, \tag{52}$$

$$\left(\mathbf{H}_0^{*T}\right)_{\mu_i\nu_j} = \left(\mathbf{H}_0^{*T}\right)^{\perp}_{\mu_i\nu_j} = {}^P\langle\mu_i|e^{-{}^*T} H_0 e^{{}^*T}|\nu_j\rangle^P. \tag{53}$$

The matrix ${}^*\mathbf{E}$ is diagonal and contains the energies of the Hamiltonian matrix $\mathbf{H}_0^{*T}$,

$${}^*\mathbf{E} = \begin{pmatrix} {}^*E_0 & & & \\ & {}^*E_1 & & \\ & & {}^*E_2 & \\ & & & \ddots \end{pmatrix}. \tag{54}$$

The left and right eigenvectors may be written as

$$\mathbf{C}_0^{\mathrm{R}} = \begin{pmatrix} 1 \\ \mathbf{0} \end{pmatrix}, \tag{55}$$

$$\mathbf{C}_0^{\mathrm{L}} = \begin{pmatrix} 1 & \bar{\boldsymbol{t}} \end{pmatrix}, \tag{56}$$

$$\mathbf{C}_n^{\mathrm{R}} = \begin{pmatrix} -\bar{\boldsymbol{t}}\,\mathbf{R}_n \\ \mathbf{R}_n \end{pmatrix}, \tag{57}$$

$$\mathbf{C}_n^{\mathrm{L}} = \begin{pmatrix} 0 & \mathbf{L}_n \end{pmatrix}, \tag{58}$$

where

$$\left(\mathbf{H}_0^{*T}\right)^{\perp}\mathbf{R} = \mathbf{R}\,{}^*\mathbf{E}^{\perp}, \tag{59a}$$

$$\mathbf{L}\left(\mathbf{H}_0^{*T}\right)^{\perp} = {}^*\mathbf{E}^{\perp}\,\mathbf{L}, \tag{59b}$$

$$\mathbf{L}\,\mathbf{R} = \mathbf{I}, \tag{59c}$$

and ${}^*\mathbf{E}^{\perp}$ is the parent-space orthogonal complement sub-block of ${}^*\mathbf{E}$ [Eq. (54)], and

$$\bar{\boldsymbol{t}}\left(\left(\mathbf{H}_0^{*T}\right)^{\perp} - {}^*E_0\mathbf{I}\right) = -{}^P\boldsymbol{\eta}. \tag{60}$$

Using Eqs. (55)–(58), the right and left eigenstates of the Hamiltonian H_0 may in the parent space be expressed in the bra-ket notation as

$$|\mathcal{B}^d\rangle = \left\{ |\mathrm{CC}^*\rangle, |0_1^*\rangle, |0_2^*\rangle, \cdots \right\}, \tag{61a}$$

$$\langle\mathcal{B}^d| = \left\{ \langle\mathrm{CC}^*|, \langle 0_1^*|, \langle 0_2^*|, \cdots \right\}, \tag{61b}$$

where

$$|\mathrm{CC}^*\rangle = e^{{}^*T}|\mathrm{HF}\rangle, \tag{62}$$

$$\langle\mathrm{CC}^*| = \langle\mathrm{HF}|e^{-{}^*T} + \sum_{\mu_i}\bar{t}_{\mu_i}\langle\mu_i|e^{-{}^*T}, \tag{63}$$

and, for $n \neq 0$,

$$|0_n^*\rangle = -\left(\sum_{\mu_i}\bar{t}_{\mu_i}\,R_{\mu_i n}\right)e^{{}^*T}|\mathrm{HF}\rangle + \sum_{\mu_i} e^{{}^*T}|\mu_i\rangle\,R_{\mu_i n}, \tag{64}$$

$$\langle 0_n^*| = \sum_{\mu_i} L_{n\mu_i}\,\langle\mu_i|e^{-T_0}. \tag{65}$$

The parent-state Jacobian in Eq. (36) may be expressed as

$$\mathbf{J}^P = \left(\mathbf{H}_0^{*T}\right)^{\perp} - {}^*E_0\mathbf{I}, \tag{66}$$

where we have used Eqs. (50) and (53). Using Eq. (66), we may write Eqs. (59a) and (59b) as

$$\mathbf{J}^P\,\mathbf{R} = \mathbf{R}\,\boldsymbol{\Omega}, \tag{67a}$$

$$\mathbf{L}\,\mathbf{J}^P = \boldsymbol{\Omega}\,\mathbf{L}, \tag{67b}$$

where

$$\boldsymbol{\Omega} = {}^*\mathbf{E}^{\perp} - {}^*E_0\mathbf{I} = \begin{pmatrix} {}^*\omega_1 & & & \\ & {}^*\omega_2 & & \\ & & {}^*\omega_3 & \\ & & & \ddots \end{pmatrix}, \tag{68}$$

with

$${}^*\omega_n = {}^*E_n - {}^*E_0. \tag{69}$$

Equations (67)–(69) show that the eigenvalues of $\mathbf{J}^P$ are equal to excitation energies in the basis of Eqs. (47). Furthermore, the derivation shows that solving the parent-space Jacobian eigenvalue equation in Eqs. (67a) and (59c) is equivalent to solving the Hamiltonian eigenvalue equation in Eq. (48).

The zeroth-order component in the parent-state Jacobian partitioning scheme [i.e., $\mathbf{A}^{(0)}$ of Eq. (46)] contains the parent-state Jacobian, $\mathbf{J}^P$, of Eq. (36). The $\mathbf{A}^{(0)}$ matrix keeps its block-diagonal structure when a bi-orthonormal transformation satisfying Eq. (59c) is carried out in the bi-orthonormal basis in Eqs. (45). When the parent state Jacobian partitioning scheme is used, the energy contributions at each order therefore are invariant with respect to the basis transformation satisfying Eq. (59c).

One of the bi-orthonormal basis transformations satisfying Eq. (59c) is described by the parent sub-space bi-orthonormal eigenstate basis in Eqs. (61). CP perturbation theory using the parent-state Jacobian partitioning scheme may therefore also be expressed in the bi-orthonormal basis

$$|\mathcal{B}^{*T}_{\mathrm{Dia}}\rangle = \left\{|\mathrm{CC}^*\rangle, |0^*_1\rangle, |0^*_2\rangle, \ldots, \mathrm{e}^{*T}|\mu_i\rangle^A\right\}, \tag{70a}$$

$$\langle\mathcal{B}^{*T}_{\mathrm{Dia}}| = \left\{\langle\mathrm{CC}^*|, \langle 0^*_1|, \langle 0^*_2|, \ldots, {}^A\langle\mu_i|\mathrm{e}^{-*T}\right\}, \tag{70b}$$

where the parent-parent block of $\mathbf{A}^{(0)}$ in Eq. (46) is diagonal and contains parent-space excitation energies on the diagonal. In practice, it is computationally most efficient to express the parent-state Jacobian partitioning scheme in the elementary basis of Eqs. (45).

We have previously shown that the parent-state Jacobian partitioning scheme leads to a perturbation expansion for the energy where the zeroth-order term is the parent-state energy and where the series formally converge to the energy of the target state. For the parent-state Jacobian partitioning, we can also determine a perturbation series for a molecular property where the zeroth-order term is the parent-state molecular property and where the series formally converge to the target-state molecular properties. This can be accomplished since response function theory is used to determine molecular properties. In particular, the response functions for the target state can be determined by expanding the time evolution of the target state in the bi-orthonormal basis in Eq. (70), while the response functions for the parent state can be determined by neglecting the auxiliary space components in this basis. When the parent-state Jacobian partitioning is used, we can thus for both the target-state energy and for the target-state molecular properties determine the parent-state energy and the parent-state molecular properties by neglecting the auxiliary space components in the bi-orthonormal basis in Eq. (70). Therefore, the strategy that we have used for determining the perturbation series for the energy can also be applied to determine perturbation series for molecular properties. When the time evolution of the target state is exponentially parameterized, the parent-state molecular properties become the ones of standard coupled cluster theory,[28] whereas for a linearly parameterized time evolution, the parent-state molecular properties become EOM-CC molecular properties.[25,26]

H. Notation for CP models

CP models are characterized by a CC parent state that is defined in the parent excitation space and by an auxiliary excitation space. This may be expressed using a notation where the parent excitation space is followed by the auxiliary excitation space in parentheses. For example, CPSD(T) denotes a CP model with a CCSD parent state and a triples auxiliary space. Furthermore, we let the notation CPSD(T) imply that the CP target state is exponentially parameterized and that molecular properties are determined from a time-evolving target state, which is also exponentially parameterized. If the time evolution is linearly parameterized, EOM-CC molecular properties are obtained and the CP model will be labeled with an overline. For example, $\overline{\mathrm{CPSD(T)}}$ denotes that energy corrections are determined using an exponential parameterization of the target state, while molecular properties are determined using a linear parameterization to describe the time evolution of the target state. If the auxiliary excitation space is followed by a number, as for example in $\overline{\mathrm{CPSD(T\text{-}3)}}$, the number denotes that perturbation corrections are determined through that order. The notation we have introduced for CP series for the energy and molecular properties describes a generalization of the notation that has previously been used to characterize energy series of CCPT theory. For example, E-CCSD(T-n) and L-CCSD(T-n) have been used to label the CCPT energy series[11] and CCPT Lagrangian series,[9] respectively, where the parent state contains the singles-and-doubles excitation space and the target state in addition contains triples excitations.

III. ENERGY CORRECTIONS FOR CP MODELS

A. Lowest-order energy corrections for the CPSD(T-n) model

As an illustration of the series of energy corrections obtained in CP theory, we consider the lowest-order energy and amplitude corrections for the CPSD(T-n) model, in which corrections to the CCSD energy are evaluated and formally converge to the CCSDT energy. We determine the amplitude corrections that are needed to evaluate the energy corrections through fifth order. The parent-state Jacobian $J^P_{\mu_i\nu_j}$ of Eq. (36) becomes the standard CCSD Jacobian, $J^{\mathrm{CCSD}}_{\mu_i\nu_j}$. Using Eqs. (35), we obtain the wave-function corrections,

$$\delta t^{(1)}_{\mu_i} = 0, \qquad i = 1, 2, \tag{71a}$$

$$\varepsilon_{\mu_3}\delta t^{(1)}_{\mu_3} = -\langle\mu_3|\Phi^{*T}|\mathrm{HF}\rangle, \tag{71b}$$

$$\begin{aligned}\sum_{j=1}^{2}\sum_{\nu_j} J^{\mathrm{CCSD}}_{\mu_i\nu_j}\delta t^{(2)}_{\nu_j} &= -\sum_{\nu_3} A^{(1)}_{\mu_i\nu_3}\delta t^{(1)}_{\nu_3} \\ &= -\sum_{\nu_3}\langle\mu_i|\left[\Phi^{*T}, \theta_{\nu_3}\right]|\mathrm{HF}\rangle\delta t^{(1)}_{\nu_3}, \quad i = 1, 2,\end{aligned} \tag{72a}$$

$$\varepsilon_{\mu_3}\delta t^{(2)}_{\mu_3} = -\sum_{\nu_3}\langle\mu_3|\left[\Phi^{*T}, \theta_{\nu_3}\right]|\mathrm{HF}\rangle\delta t^{(1)}_{\nu_3}, \tag{72b}$$

$$\begin{aligned}\sum_{j=1}^{2}\sum_{\nu_j} J^{\mathrm{CCSD}}_{\mu_i\nu_j}\delta t^{(3)}_{\nu_j} &= -\sum_{j=1}^{3}\sum_{\nu_j} A^{(1)}_{\mu_i\nu_j}\delta t^{(2)}_{\nu_j} \\ &= -\sum_{\nu_3}\langle\mu_i|\left[\Phi^{*T}, \theta_{\nu_3}\right]|\mathrm{HF}\rangle\delta t^{(2)}_{\nu_3}, \quad i = 1, 2,\end{aligned} \tag{73a}$$

$$\varepsilon_{\mu_3}\delta t^{(3)}_{\mu_3} = -\sum_{j=1}^{3}\sum_{\nu_j}\langle\mu_3|\left[\Phi^{*T}, \theta_{\nu_j}\right]|\mathrm{HF}\rangle\delta t^{(2)}_{\nu_j}, \tag{73b}$$

$$\begin{aligned}\sum_{j=1}^{2}\sum_{\nu_j} J^{\mathrm{CCSD}}_{\mu_i\nu_j}\delta t^{(4)}_{\nu_j} &= -\sum_{\nu_3}\langle\mu_i|\left[\Phi^{*T}, \theta_{\nu_3}\right]|\mathrm{HF}\rangle\delta t^{(3)}_{\nu_3} \\ &\quad -\langle\mu_i|\left[\left[\Phi^{*T}, \delta T^{(2)}_1\right], \delta T^{(1)}_3\right]|\mathrm{HF}\rangle\delta_{i2}, \; i = 1, 2.\end{aligned} \tag{74}$$

The energy corrections through the fifth order may be obtained from Eqs. (41)–(44) and become

$$E_0^{(0)} = {}^*E_0 = \langle \mathrm{HF}|H_0^{*T}|\mathrm{HF}\rangle, \tag{75}$$

$$E_0^{(1)} = 0, \tag{76}$$

$$E_0^{(2)} = 0, \tag{77}$$

$$E_0^{(3)} = \langle \mathrm{HF}|\left[\Phi^{*T}, \delta T_1^{(2)} + \delta T_2^{(2)}\right]|\mathrm{HF}\rangle, \tag{78}$$

$$E_0^{(4)} = \langle \mathrm{HF}|\left[\Phi^{*T}, \delta T_1^{(3)} + \delta T_2^{(3)}\right]|\mathrm{HF}\rangle, \tag{79}$$

$$E_0^{(5)} = \langle \mathrm{HF}|\left[\Phi^{*T}, \delta T_1^{(4)} + \delta T_2^{(4)}\right]|\mathrm{HF}\rangle + \frac{1}{2}\langle \mathrm{HF}|\left[\left[\Phi^{*T}, \delta T_1^{(2)}\right], \delta T_1^{(2)}\right]|\mathrm{HF}\rangle. \tag{80}$$

Let us examine the lowest-order energy contributions in more detail. To do this, we use Eqs. (72a), (73a), and (74) to rewrite $E_0^{(3)}$, $E_0^{(4)}$, and $E_0^{(5)}$ as

$$E_0^{(3)} = -\sum_{i,j=1}^{2}\sum_{\mu_i\nu_j\lambda_3}\langle \mathrm{HF}|\left[\Phi^{*T}, \theta_{\mu_i}\right]|\mathrm{HF}\rangle\left(\boldsymbol{J}^{\mathrm{CCSD}}\right)^{-1}_{\mu_i\nu_j} \times \langle \nu_j|\left[\Phi^{*T}, \theta_{\lambda_3}\right]|\mathrm{HF}\rangle\delta t_{\lambda_3}^{(1)}, \tag{81}$$

$$E_0^{(4)} = -\sum_{i,j=1}^{2}\sum_{\mu_i\nu_j\lambda_3}\langle \mathrm{HF}|\left[\Phi^{*T}, \theta_{\mu_i}\right]|\mathrm{HF}\rangle\left(\boldsymbol{J}^{\mathrm{CCSD}}\right)^{-1}_{\mu_i\nu_j} \times \langle \nu_j|\left[\Phi^{*T}, \theta_{\lambda_3}\right]|\mathrm{HF}\rangle\delta t_{\lambda_3}^{(2)}, \tag{82}$$

$$\begin{aligned} E_0^{(5)} = &-\sum_{i,j=1}^{2}\sum_{\mu_i\nu_j\lambda_3}\langle \mathrm{HF}|\left[\Phi^{*T}, \theta_{\mu_i}\right]|\mathrm{HF}\rangle\left(\boldsymbol{J}^{\mathrm{CCSD}}\right)^{-1}_{\mu_i\nu_j} \times \langle \nu_j|\left[\Phi^{*T}, \theta_{\lambda_3}\right]|\mathrm{HF}\rangle\delta t_{\lambda_3}^{(3)} \\ &-\sum_{i,j=1}^{2}\sum_{\mu_i\nu_j}\langle \mathrm{HF}|\left[\Phi^{*T}, \theta_{\mu_i}\right]|\mathrm{HF}\rangle\left(\boldsymbol{J}^{\mathrm{CCSD}}\right)^{-1}_{\mu_i\nu_j} \times \langle \nu_j|\left[\left[\Phi^{*T}, \delta T_1^{(2)}\right], \delta T_3^{(1)}\right]|\mathrm{HF}\rangle \\ &+\frac{1}{2}\langle \mathrm{HF}|\left[\left[\Phi^{*T}, \delta T_1^{(2)}\right], \delta T_1^{(2)}\right]|\mathrm{HF}\rangle. \end{aligned} \tag{83}$$

$E_0^{(3)}$ in Eq. (81) shows how the effect of triples, as expressed by $\delta t_{\lambda_3}^{(1)}$, is projected into the singles-and-doubles space to obtain the leading-order triples energy contribution. Similarly, $E_0^{(4)}$ in Eq. (82) shows how the effect of *relaxed* triples, as expressed by $\delta t_{\lambda_3}^{(2)}$, is projected into the singles-and-doubles space to obtain the energy contribution originating from the relaxed triples. The first term of $E_0^{(5)}$ in Eq. (83) describes, in a similar way, how triples amplitudes that are further relaxed, as expressed by $\delta t_{\lambda_3}^{(3)}$, are projected into the singles-and-doubles space to obtain the corresponding triples-relaxed energy contribution. Note that while the $\delta t_{\lambda_3}^{(2)}$ triples relaxation contribution is due to an internal relaxation in the triples space [the sum in Eq. (72b) runs only through the triples space], the relaxation in the $\delta t_{\lambda_3}^{(3)}$ triples contribution is referencing also the singles-and-doubles space [the sum in Eq. (73b) runs through the singles-and-doubles and triples spaces]. The last two terms of $E_0^{(5)}$ contain connected energy contributions.

B. Comparison of the CPSD(T-n) and the L-CCSD(T-n) energy series

In CCPT theory, two energy series—the CCPT energy series[11] and the CCPT Lagrangian series[9]—have previously been developed, where energy corrections are determined in orders of Φ^{*T}, the zeroth-order term is the energy of the CC parent state, and the series converge to the energy of the CC target state. The CCPT energy series[11] may be obtained as described in Sec. II in Eqs. (31)–(33). The CCPT Lagrangian series[9] may be determined by parameterizing the energy Lagrangian for the CC target state with the CC parent state and its bi-orthonormal parent multiplier state as the expansion point. For the CCPT energy and CCPT Lagrangian series, we use a notation similar to the one we have used for the CP models, where the label CP is replaced by the label E-CC for the CCPT energy series and with the label L-CC for the CCPT Lagrangian series. For example, CPSD(T-n), E-CCSD(T-n), and L-CCSD(T-n) denote CP, CCPT energy, and CCPT Lagrangian series, respectively, with a CCSD parent state targeting the energy of a CCSDT state. We will in this section compare the energy corrections for the CPSD(T-n) and L-CCSD(T-n) series. The L-CCSD(T-n) series is given in Ref. 9. In order to compare the energy contributions of the L-CCSD(T-n) with the CPSD(T-n) series, we rewrite $E_0^{(3)}$, $E_0^{(4)}$, and $E_0^{(5)}$ in Eqs. (81)–(83) using the CCSD multiplier equation,

$$\sum_{i=1}^{2}\sum_{\mu_i}{}^*\bar{t}_{\mu_i}J^{\mathrm{CCSD}}_{\mu_i\nu_j} = -\langle \mathrm{HF}|\left[\Phi^{*T}, \theta_{\nu_j}\right]|\mathrm{HF}\rangle, \qquad j = 1, 2, \tag{84}$$

where ${}^*\bar{t}_{\mu_i}$, $i = 1, 2$, denotes CCSD multipliers. Substituting Eq. (84) in Eqs. (81)–(83) gives

$$E_0^{(3)} = \sum_{i=1}^{2}\sum_{\mu_i\nu_3}{}^*\bar{t}_{\mu_i}\langle \mu_i|\left[\Phi^{*T}, \theta_{\nu_3}\right]|\mathrm{HF}\rangle\delta t_{\nu_3}^{(1)}, \tag{85}$$

$$E_0^{(4)} = \sum_{i=1}^{2}\sum_{\mu_i\nu_3}{}^*\bar{t}_{\mu_i}\langle \mu_i|\left[\Phi^{*T}, \theta_{\nu_3}\right]|\mathrm{HF}\rangle\delta t_{\nu_3}^{(2)}, \tag{86}$$

$$E_0^{(5)} = E_0^{(5)}(\mathrm{T}) + E_0^{(5)}(\mathrm{ST}) + E_0^{(5)}(\mathrm{SS}), \tag{87}$$

where

$$E_0^{(5)}(\mathrm{T}) = \sum_{i=1}^{2}\sum_{\mu_i\nu_3}{}^*\bar{t}_{\mu_i}\langle \mu_i|\left[\Phi^{*T}, \theta_{\nu_3}\right]|\mathrm{HF}\rangle\delta t_{\nu_3}^{(3)}, \tag{88}$$

$$E_0^{(5)}(\mathrm{ST}) = \sum_{j=1}^{2}\sum_{\nu_j}{}^*\bar{t}_{\nu_j}\langle \nu_j|\left[\left[\Phi^{*T}, \delta T_1^{(2)}\right], \delta T_3^{(1)}\right]|\mathrm{HF}\rangle, \tag{89}$$

$$E_0^{(5)}(\mathrm{SS}) = \frac{1}{2}\langle \mathrm{HF}|\left[\left[\Phi^{*T}, \delta T_1^{(2)}\right], \delta T_1^{(2)}\right]|\mathrm{HF}\rangle. \tag{90}$$

Substituting Eq. (73b) in Eq. (88) gives

$$E_0^{(5)}(\mathrm{T}) = -\sum_{i=1}^{2}\sum_{j=1}^{3}\sum_{\mu_i\lambda_j\nu_3} {}^{*}\bar{t}_{\mu_i}\langle\mu_i|\big[\Phi^{*T},\theta_{\nu_3}\big]|\mathrm{HF}\rangle\varepsilon_{\nu_3}^{-1} \times \langle\nu_3|\big[\Phi^{*T},\theta_{\lambda_j}\big]|\mathrm{HF}\rangle\delta t_{\lambda_j}^{(2)}. \quad (91)$$

Introducing the first-order multipliers of Eq. (2.29a) in Ref. 9 as

$$\delta\bar{t}_{\nu_3}^{(1)} = -\varepsilon_{\nu_3}^{-1}\sum_{i=1}^{2}\sum_{\mu_i} {}^{*}\bar{t}_{\mu_i}\langle\mu_i|\big[\Phi^{*T},\theta_{\nu_3}\big]|\mathrm{HF}\rangle, \quad (92)$$

we may write Eq. (91) as

$$E_0^{(5)}(\mathrm{T}) = \sum_{j=1}^{3}\sum_{\lambda_j\nu_3}\delta\bar{t}_{\nu_3}^{(1)}\langle\nu_3|\big[\Phi^{*T},\theta_{\lambda_j}\big]|\mathrm{HF}\rangle\delta t_{\lambda_j}^{(2)} = E_0^{(5)}(\mathrm{T\text{-}S}) + E_0^{(5)}(\mathrm{T\text{-}D}) + E_0^{(5)}(\mathrm{T\text{-}T}), \quad (93)$$

where

$$E_0^{(5)}(\mathrm{T\text{-}S}) = \sum_{\nu_3}\delta\bar{t}_{\nu_3}^{(1)}\langle\nu_3|\big[\Phi^{*T},\delta T_1^{(2)}\big]|\mathrm{HF}\rangle, \quad (94)$$

$$E_0^{(5)}(\mathrm{T\text{-}D}) = \sum_{\nu_3}\delta\bar{t}_{\nu_3}^{(1)}\langle\nu_3|\big[\Phi^{*T},\delta T_2^{(2)}\big]|\mathrm{HF}\rangle, \quad (95)$$

$$E_0^{(5)}(\mathrm{T\text{-}T}) = \sum_{\nu_3}\delta\bar{t}_{\nu_3}^{(1)}\langle\nu_3|\big[\Phi^{*T},\delta T_3^{(2)}\big]|\mathrm{HF}\rangle. \quad (96)$$

The lowest non-vanishing contribution in the L-CCSD(T-n) series enters in second-order and is given in Eq. (3.1a) of Ref. 10. The L-CCSD(T-2) energy correction is in Ref. 10 denoted by $E_{\mathrm{T\text{-}2}}^{(2)}$, and a comparison with $E_0^{(3)}$ of Eq. (85) shows

$$E_{\mathrm{T\text{-}2}}^{(2)} = E_0^{(3)}. \quad (97)$$

The L-CCSD(T-3) energy contribution is given in Eq. (3.1b) of Ref. 10 and is denoted by $E_{\mathrm{T\text{-}3}}^{(3)}$. A comparison with $E_0^{(4)}$ of Eq. (86) shows

$$E_{\mathrm{T\text{-}3}}^{(3)} = E_0^{(4)}. \quad (98)$$

The L-CCSD(T-4) energy contribution is given in Eq. (2.33) of Ref. 9 as

$$E_{\mathrm{T\text{-}4}}^{(4)} = \sum_{\mu_2} {}^{*}\bar{t}_{\mu_2}\langle\mu_2|\big[\big[\Phi,\delta T_3^{(1)}\big],\delta\widetilde{T}_1^{(2)}\big]|\mathrm{HF}\rangle + \sum_{\nu_3}\delta\bar{t}_{\nu_3}^{(1)}\langle\nu_3|\big[\Phi^{*T},\delta\widetilde{T}_1^{(2)}+\delta\widetilde{T}_2^{(2)}+\delta T_3^{(2)}\big]|\mathrm{HF}\rangle, \quad (99)$$

where the notation of the present article is used and where the singles and doubles second-order cluster operators are given as

$$\delta\widetilde{T}_i^{(2)} = \sum_{\mu_i}\delta\widetilde{t}_{\mu_i}^{(2)}\theta_{\mu_i}, \qquad i=1,2, \quad (100)$$

with the amplitudes

$$\delta\widetilde{t}_{\mu_i}^{(2)} = -\varepsilon_{\mu_i}^{-1}\langle\mu_i|\big[\Phi^{*T},\delta T_3^{(1)}\big]|\mathrm{HF}\rangle, \qquad i=1,2. \quad (101)$$

The $\delta\widetilde{t}_{\mu_1}^{(2)}$ and $\delta\widetilde{t}_{\mu_2}^{(2)}$ amplitudes of Eq. (101) may be obtained from the ones in Eq. (72a) by replacing the CCSD Jacobian in Eq. (72a) with a diagonal matrix containing orbital energy differences. Comparing $E_{\mathrm{T\text{-}4}}^{(4)}$ of Eq. (99) with $E_0^{(5)}$ of Eqs. (87)–(90) and (93)–(96), we identify the triples amplitudes contribution to the second term of Eq. (99) with the triples-triples term in Eq. (93),

$$E_0^{(5)}(\mathrm{T\text{-}T}) = \sum_{\nu_3}\delta\bar{t}_{\nu_3}^{(1)}\langle\nu_3|\big[\Phi^{*T},\delta T_3^{(2)}\big]|\mathrm{HF}\rangle, \quad (102)$$

while the remaining terms in $E_{\mathrm{T\text{-}4}}^{(4)}$ can be obtained from the $E_0^{(5)}(\mathrm{T\text{-}S})$, $E_0^{(5)}(\mathrm{T\text{-}D})$, and $E_0^{(5)}(\mathrm{ST})$ contributions to $E_0^{(5)}$ by replacing the $\delta t_{\mu_1}^{(2)}$ and $\delta t_{\mu_2}^{(2)}$ amplitudes of Eq. (72a) with the amplitudes of Eq. (101). In addition, $E_0^{(5)}$ contains the $E_0^{(5)}(\mathrm{SS})$ contribution which has no counterpart in $E_{\mathrm{T\text{-}4}}^{(4)}$.

The two lowest non-vanishing order contributions in the L-CCSD(T-n) and CPSD(T-n) series are thus identical. However, the L-CCSD(T-n) series starts at second order, whereas the CPSD(T-n) series starts at third order. This difference in counting orders is due to the fact that the multipliers for the CCSD reference state are assigned no order in the L-CCSD(T-n) series,[9] whereas for the CPSD(T-n) series, they are assigned one order in Φ^{*T} as the right-hand side of the multiplier equations contains a Φ^{*T} perturbation operator; see Eq. (84). All the $E_{\mathrm{T\text{-}4}}^{(4)}$ terms in Eq. (99) have counterparts in the $E_0^{(5)}$ in Eq. (87), where the $E_{\mathrm{T\text{-}4}}^{(4)}$ terms are obtained from the $E_0^{(5)}$ terms by replacing the internally relaxed second-order singles and doubles amplitudes in Eq. (72a) with the internally *unrelaxed* second-order singles and doubles amplitudes of Eq. (101). In addition, the energy contribution in Eq. (87) contains the $E_0^{(5)}(\mathrm{SS})$ term. As the $E_0^{(5)}(\mathrm{SS})$ term does not contain the CCSD multipliers, this term will appear as a fifth-order term in the L-CCSD(T-n) series.

For the CPSD(T-n) series, the two lowest energy corrections are identical to the two lowest energy corrections in the L-CCSD(T-n) series, with the order increased by one in the CPSD(T-n) series. In general, for a fixed parent and target excitation space, the two lowest energy corrections are equal in the CP and CCPT Lagrangian series, with the CP corrections formally being one order higher than in the CCPT Lagrangian series. In the numerical section, Sec. V, to facilitate a direct comparison of the convergence of the CP and the CCPT Lagrangian series, we have adjusted the order of the CCPT Lagrangian series by one to have identical energy contributions in the two series in the first two orders.

IV. MATHEMATICAL CONSIDERATIONS ON THE CONVERGENCE OF PERTURBATION THEORY

Before discussing the convergence of CP ground-state energy series for various choices of parent and target states, we briefly review the general theory of convergence for perturbation theory in finite-dimensional spaces. A comprehensive discussion of the general theory of the convergence for the CP series for the ground-state energy and for molecular properties, including excitation energies, can be found in Paper IV.[15] We first introduce the mathematical formalism that is needed to establish whether a perturbation expansion is convergent and then apply this formalism to a simple two-state model, which may be used for analyzing the convergence behavior of finite-dimensional perturbation expansions. The premises for setting up the two-state model and for using it to examine the convergence of perturbation series have been studied in Paper IV[15] and in Ref. 16. In the latter article, the two-state model has been examined in detail and the convergence rate and the convergence patterns that

may arise for a two-state problem have been determined. In Subsection IV C, we introduce the five archetypes that cover the convergence patterns, which can be encountered for ground-state energy perturbation series that effectively become a two-state problem at high orders.

A. General considerations

Consider a general perturbation partitioning of a Hamiltonian matrix $\mathbf{H}$ into a zeroth-order matrix $\mathbf{H}_0$ and a perturbation $\mathbf{V}$,

$$\mathbf{H}(z) = \mathbf{H}_0 + z\mathbf{V}, \tag{103}$$

where z is the perturbation parameter, which may be complex. The eigenvalues and eigenvectors of $\mathbf{H}(z)$ are functions of z, so we may write the eigenvalue equation for $\mathbf{H}(z)$ as

$$\mathbf{H}(z)\mathbf{X}(z) = E(z)\mathbf{X}(z), \tag{104}$$

where $E(z)$ and $\mathbf{X}(z)$ are the z-dependent eigenvalue and eigenvector, respectively. Assuming that the unperturbed eigenvalue of $\mathbf{H}_0$ is non-degenerate, the function $E(z)$ is analytic in the region around $z = 0$ where $E(z)$ is non-degenerate. The perturbation expansion for the eigenvalue of interest, $E = E(1)$, is thus convergent if $E(z)$ is analytic within the complex unit circle, $|z| \leq 1$. The question of convergence or divergence of a perturbation expansion may therefore be settled by examining the eigenvalue $E(z)$ as a function of z and determining the lowest value of $|z|$ for which $E(z)$ is degenerate. We will call this point of degeneracy the *primary critical point*, so the perturbation expansion is divergent if the primary critical point is inside the complex unit circle and convergent if the point is outside.

An eigenstate $\mathbf{Y}(z)$ that becomes degenerate with $\mathbf{X}(z)$ for $|z| < 1$ is called an intruder state. If the degeneracy occurs for a negative value of the real part of z, then the intruder state is a back-door intruder, whereas the occurrence of the degeneracy for a positive value corresponds to a front-door intruder. We will see below that the location of the primary stationary point in the positive or negative half plane is directly related to the signs of the higher-order corrections.

The above discussion relates to the standard perturbation expansion of an eigenvalue problem. However, CP perturbation theory is connected to an expansion of a set of non-linear equations and it is therefore not evident that the standard mathematical theory of perturbation expansion applies to the present case. In connection to the development of CCPT perturbation theory, we have discussed the formal requirements for convergence of such perturbation expansions and have shown that the intruder states occur as excitation operators that give singularities of the perturbation-dependent Jacobian within the unit circle.[14] For CP theory, we have in Paper IV[15] examined the theoretical foundation for having convergent CP perturbation series both for the ground-state energy and for molecular properties, including excitation energies. With the modification that the determination of degeneracies for the energy is replaced by a determination of singularities of the perturbation-dependent Jacobian, we will use the standard terms, such as back- and front-door intruders, also for perturbation expansions that are obtained using CCPT and CP theories.

B. The two-state model

When the high-order MPPT corrections to the wave function are examined, it is found that these corrections become nearly linearly dependent[29,30] and may therefore be written in terms of a single vector. Furthermore, for MPPT, this vector has been found to be identical to the eigenvector that leads to the primary critical point. The higher-order corrections in MPPT may therefore be understood in terms of a two-dimensional space containing the two degenerate states of the primary critical point. For the CP and CCPT expansions, the overlaps between the various corrections to the excitation operator have also been analyzed,[16] and it has been found that these corrections also approach a one-dimensional ray and may therefore also be studied using a two-dimensional model containing two degenerate states of the primary critical point.

To set up the two-dimensional model, we will use for the two-dimensional space the same notation as for the full dimensional space and assume that the basis vectors of the two-dimensional space are orthonormal and diagonalize the zeroth-order Hamiltonian. The zeroth-order Hamiltonian and the perturbation may then be written as[16,30]

$$\mathbf{H}_0 = \begin{pmatrix} \alpha & 0 \\ 0 & \beta + \gamma \end{pmatrix}, \tag{105}$$

$$\mathbf{V} = \begin{pmatrix} 0 & \delta_1 \\ \delta_2 & -\gamma \end{pmatrix}, \tag{106}$$

where α and $\beta + \gamma$ are the two zeroth-order energies, and γ and δ_1, δ_2 are the gap shift and the coupling terms, respectively. We will in the following assume that the $\beta > \alpha$ and $\beta + \gamma > \alpha$, so the numerical order of the diagonal terms is the same in $\mathbf{H}_0$ and $\mathbf{H}_0 + \mathbf{V}$. Notice also that the perturbation is not necessarily Hermitian, as the coupling terms, δ_1 and δ_2, may differ. The general form of the perturbation allows the model to describe general perturbation expansions as occurring in, for example, coupled cluster theory and multi-state perturbation expansions.

The two eigenvalues of the matrix $\mathbf{H}_0 + z\mathbf{V}$ are determined as[16,30]

$$E_\pm(z) = \frac{\alpha + \beta + (1-z)\gamma}{2} \pm \frac{\sqrt{(\alpha - \beta - (1-z)\gamma)^2 + 4\delta_1\delta_2 z^2}}{2}. \tag{107}$$

Equation (107) shows that the eigenvalues, as functions of z, depend on the product $\delta_1\delta_2$ and not on the individual coupling elements. We may therefore replace the individual coupling coefficients with a positive geometric average of these, δ, and a symmetry factor, σ,

$$\delta = \sqrt{|\delta_1\delta_2|} \tag{108}$$

$$\sigma = \begin{cases} +1, & \text{if } \delta_1\delta_2 \geq 0 \\ -1, & \text{if } \delta_1\delta_2 < 0, \end{cases} \tag{109}$$

so

$$\delta_1\delta_2 = \sigma\delta^2. \tag{110}$$

The eigenvalues of Eq. (107) may therefore be written in terms of σ and δ as

$$E_\pm(z) = \frac{\alpha + \beta + (1-z)\gamma}{2} \pm \frac{\sqrt{(\alpha - \beta - (1-z)\gamma)^2 + 4\sigma\delta^2 z^2}}{2}. \tag{111}$$

The relation between the diagonal elements of $\mathbf{H}_0 + \mathbf{V}$, i.e., α and β, and the eigenvalues $E_\pm$ depends on the symmetry factor. Since the square root is a monotonically increasing function, it is first noted that $\sqrt{(\alpha-\beta)^2 + 4\sigma\delta^2}$ is larger than $|\beta - \alpha|$ for $\sigma = 1$ and smaller than $|\beta - \alpha|$ for $\sigma = -1$. The symmetric perturbation, $\sigma = 1$, leads thus to a lowest eigenvalue, E_-, that is below α and a largest eigenvalue, E_+, that is above β. For an asymmetric perturbation, $\sigma = -1$, and for $|\gamma| \leq \frac{|\beta-\alpha|}{2}$, one obtains a real lowest eigenvalue that is larger than α and a real largest eigenvalue that is lower than β, whereas for $|\gamma| > \frac{|\beta-\alpha|}{2}$, one obtains a pair of complex eigenvalues. In the present context, where we consider perturbation expansions of the ground-state energy, we have in general that the eigenvalue of interest is the lowest and that the perturbation expansion reduces the total energy. We will therefore restrict our considerations to the symmetric case, $\sigma = +1$, and use Eq. (111) with this choice of σ as the point of departure.

The primary critical points are defined by $E_-(z) = E_+(z)$, corresponding to the complex pair of parameters,

$$z^c_\pm = \frac{\beta + \gamma - \alpha}{4\delta^2 + \gamma^2}(\gamma \pm 2\delta \mathrm{i}). \tag{112}$$

The norm of the critical points is given by

$$|z^c_\pm| = \frac{\beta - \alpha + \gamma}{\sqrt{4\delta^2 + \gamma^2}}, \tag{113}$$

so the perturbation expansion is divergent if

$$\frac{(\beta - \alpha + \gamma)^2}{4\delta^2 + \gamma^2} < 1. \tag{114}$$

In Ref. 16, it is shown that the asymptotic rate of convergence, r, and the norm of the critical point are inverses of each other,

$$r = \frac{1}{|z^c|}, \tag{115}$$

so the location of the critical point does not only define whether the expansion is convergent or divergent, but it also defines the rate of convergence for a convergent expansion.

Since $\beta + \gamma - \alpha$ is positive by assumption, it is seen from Eq. (112) that the sign of the gap shift defines the position of the critical points in the complex plane: a positive gap shift leads to a critical point being located in the half plane with positive real values,

TABLE I. Archetypes of convergence patterns for two-state perturbation expansions (see text for details).

Archetype	Geometric	Ripples
Identification	$\|\gamma\| \gg \|\delta\|$	$\|\gamma\| > \|\delta\|$
	Typical absolute corrections and deviations	
	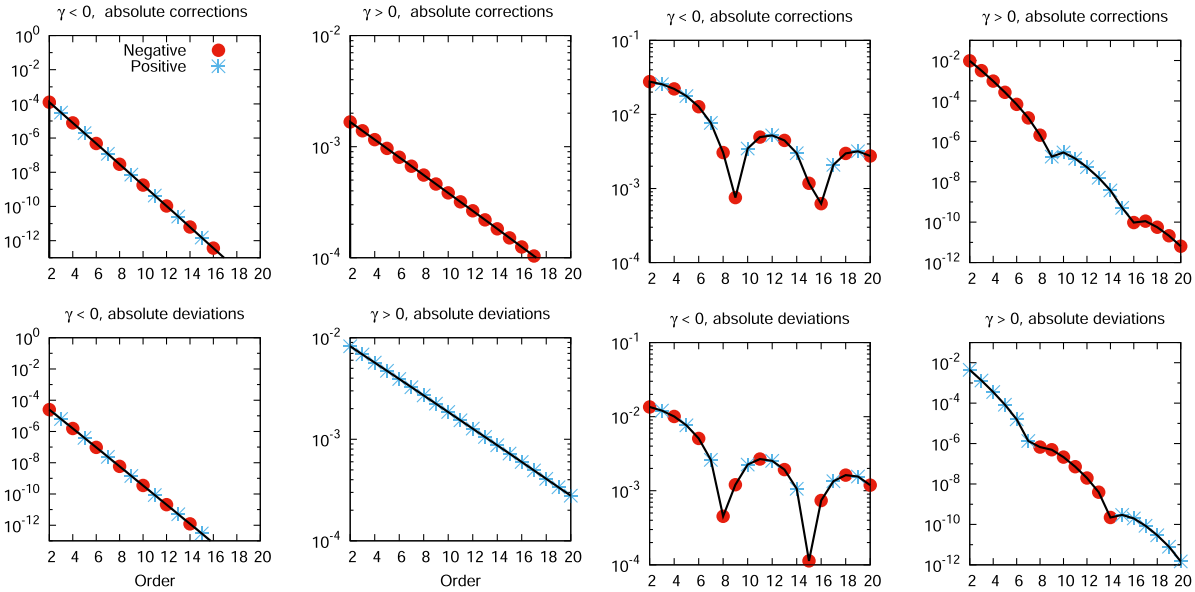	
Sign pattern of corrections	$\gamma < 0 : (1+, 1-)$ $\gamma > 0 : (-)$	$\gamma < 0 : (1+, 1-)$ $\gamma > 0 : (n^*-, n^*+)$
Period n^*	...	$2.5 + \sqrt{2}\left\|\frac{\gamma}{\delta}\right\|$

whereas a negative gap shift leads to a critical point in the negative half plane. Similarly, an intruder state for a Hamiltonian with a positive gap shift is necessarily a front-door intruder, whereas an intruder state for a negative gap shift is a back-door intruder.

C. Archetypes of convergence

In Ref. 16, we have analyzed the form of the energy corrections for the two-state perturbation expansion for general choices of γ, δ, and σ and have shown that there are five archetypes of convergence patterns for the considered symmetric perturbations. Of the five archetypes—zigzag, interspersed zigzag, triadic, geometric, and ripples—all but the zigzag have been observed.[16] In the present context, we are studying perturbation expansions of ground-state energies and only two of these archetypes will be encountered: geometric and ripples. The properties and typical patterns of these two archetypes are given in Table I. For both archetypes, corrections and deviations are plotted for both negative and positive gap shifts. The plots are logarithmic and a simple color code is used to differentiate between positive (blue) and negative (red) corrections and deviations. To avoid unnecessary cluttering of the plots, the color codes are defined only on the first plot. The geometric and ripples archetypes arise when the absolute value of the gap shift γ is larger than the absolute value of the coupling element δ. If the gap shift is much larger than the coupling, the archetype is geometric, where the convergence exhibits a simple geometric form. For this archetype, a positive value of the gap shift implies that all corrections are negative, which in the table is denoted by (−), whereas a negative value of the gap shift leads to corrections of alternating sign, which is denoted by (1+, 1−). The sign of the gap shift may therefore be directly deduced from the signs of the corrections. When the size of the gap shift increases toward the coupling or when larger orders are considered, the ripples pattern occurs. In the ripples pattern, there are recurring ripples that are delineated by marked local minima in the size of the corrections and deviations. The number of orders spanned by a ripple, n^*, is proportional to the ratio $|\frac{\gamma}{\delta}|$, which explains why the ripples are not observed in actual calculations when the coupling is much smaller than the gap shift. The signs of the corrections depend on the sign of the gap shift. If the gap shift is negative, the corrections and deviations have in general alternating signs, with exceptions occurring at the boundary between two ripples, where typically two corrections and two deviations have the same sign. If the gap shift is positive, all corrections have the same sign in a given ripple and the sign changes, when going from one ripple to the next. The deviations for a single ripple have similarly a common sign, which is opposite to that of the corrections for this ripple.

V. NUMERICAL RESULTS

In this section, we report calculations using the CP energy series, as well as the CCPT energy and CCPT Lagrangian series, for various CC parent and CC target states. We also report the MPPT series calculations with the FCI state as the target state. Our test examples consist of hydrogen fluoride, HF, in aug-cc-pVDZ basis at three geometries, R_e, $1.5R_e$, and $2.0R_e$, methylene, CH_2, in cc-pVTZ basis, and the fluorine anion, F^-, in aug-cc-pVTZ basis. The equilibrium geometries are those used in Ref. 14, and the 1s core orbitals are frozen for all atoms but hydrogen. The test examples have been chosen to study the convergence of CP energy series for electron-rich and electron-poor molecular systems and for various degrees of multi-configurational character of the wave function. The use of hydrogen fluoride at the three bond-distances thus allows us to study a molecule containing an electron-rich atom with various degrees of multi-configurational wave functions. At R_e, the HF molecule is strongly dominated by the Hartree-Fock configuration, at $1.5R_e$, the wave function has a minor multi-configurational component, whereas at $2.0R_e$, there is a large multi-configurational component. More quantitatively, the occupations of the anti-bonding sigma orbitals are 0.03, 0.09, and 0.26 for R_e, $1.5R_e$, and $2.0R_e$, respectively. For the methylene molecule, we are using the lowest lying closed-shell state as the reference state. The methylene molecule has a low-lying doubly excited singlet state, and because the carbon atom is not electron-rich, the high-order convergence becomes defined by a primary critical point in the positive complex half plane. Finally, the fluorine anion is electron-rich and has a low-lying excited singlet state, so the anion has either a back-door intruder or a curve-crossing slightly outside the negative part of the unit circle. As we will see below, the MPPT expansions are only convergent for one of these test cases, the methylene molecule, so this choice of test cases allows us to study the performance of CP and CCPT perturbation series for molecules for which higher-order MPPT fails.

The CP, CCPT energy, CCPT Lagrangian, and MPPT energy series calculations have been carried using the general coupled cluster codes[31] of LUCIA.[32] LUCIA has thus been extended to use the zeroth-order target-space Jacobian for both the Fock operator partitioning [Eq. (31)] and the parent-state Jacobian partitioning [Eq. (39)]. The codes developed in LUCIA allow for calculations through arbitrary order with arbitrary excitation spaces for the parent and target states. The price for this generality is that the codes are rather inefficient, making in particular high-order calculations time consuming. The atomic-orbital integrals were obtained from the standard version of DALTON.[33,34]

We have performed calculations for the CPS(D-n), CPSD(T-n), and CPSDT(Q-n) energy series, where the parent and target excitation spaces differ by a single excitation level. These calculations will be discussed in the following. In addition, we have also performed calculations using the CPS(DT-n) and CPSD(TQ-n) series, where the parent and target excitation spaces differ by two excitation levels. The latter two series will only be used to examine general convergence trends as functions of the parent and target spaces, but the performance of the individual orders for these two expansions will not be discussed. For comparison, calculations have also been performed for the standard MPPT energy series and the CCPT energy and CCPT Lagrangian series using the above parent and target excitation spaces. The calculations were in general carried out through order 40, but for the most computationally demanding calculations containing the CCSDTQ target state, the largest order was reduced to 20 or less. Calculations were terminated if the energy corrections became smaller than 10^{-6} or larger than 1. For convergent expansions, we also determine the rate of convergence, which is defined as the ratio of the absolute energy deviations of two consecutive orders. A rate of convergence close to one thus indicates a slowly convergent series, whereas a convergence rate significantly smaller than one indicates a fast convergent series. In practice, the rate of convergence

TABLE II. Summary of the convergence behavior of the MPPT calculations.

	HF at R_e	HF at 1.5 R_e	HF at 2 R_e	CH_2	F^-
Low-order results: Fraction of full correlation energy recovered					
Order 2 (%)	96.4	96.0	93.4	81.5	98.7
Order 3 (%)	96.7	94.3	90.3	93.3	94.7
Order 4 (%)	100.4	100.7	100.6	97.1	102.1
Order 5 (%)	99.3	98.1	95.6	98.3	97.4
Order 6 (%)	100.4	101.3	103.1	98.9	102.8
High-order convergence					
Convergent?	No	No	No	Yes	No
Rate of convergence	...	...	...	0.79	...
Archetype	Geo.	Geo.	Geo.	Geo.	Geo.
Signs	(1+, 1−)	(1+, 1−)	(1+, 1−)	(−)	(1+, 1−)

was obtained from a linear least square fit of the logarithmic absolute errors for orders larger than or equal to 10.

We will examine several features of the performed calculations. First of all, we will examine the amount of differential correlation energy that the various series recover at lower order, for example, how large part of the triples correlation energy is recovered in the first five non-vanishing orders of CPSD(T-n). This aspect determines obviously the potential practical use of the new hierarchies. A more fundamental question is whether the CP series are converging in high orders and which archetype the high-order corrections correspond to. The latter provides information about the gap shift and coupling term of the perturbation and may therefore be used to design better forms of the parent space or improved perturbation methods. It is also of interest to investigate to what extent the CP hierarchy removes the divergences of MPPT that arise due to back-door intruders as these divergences drastically reduce the applicability of MPPT beyond the second order.

A. The MPPT series

Before embarking on the CP calculations, it is useful to review the calculations for the standard MPPT energy series. The MPPT series for the five test cases are summarized in Table II and Fig. 1. The figure displays logarithmic plots of the absolute deviations

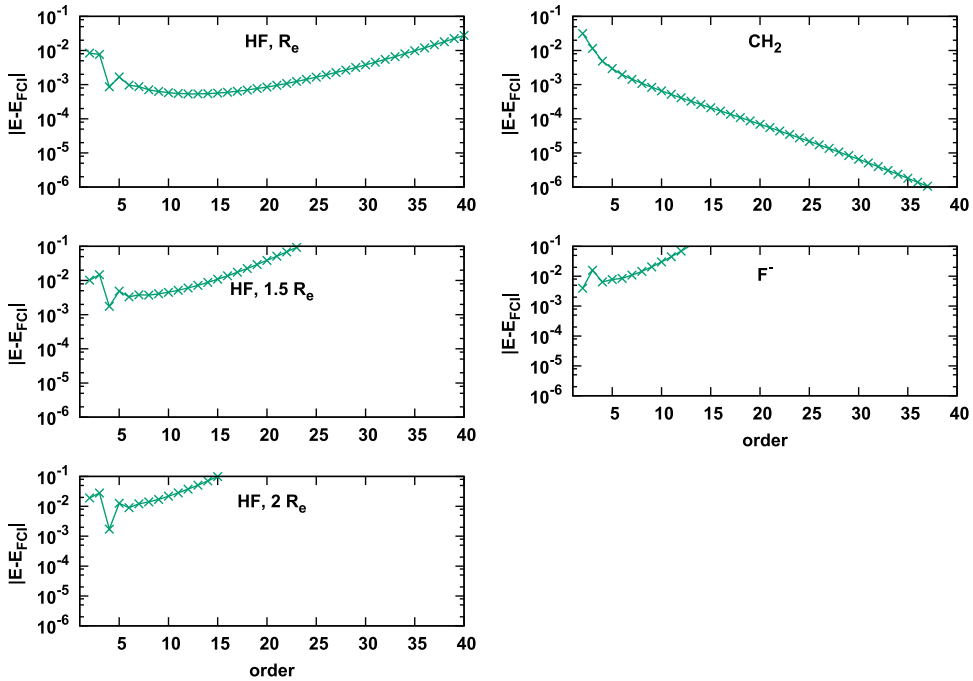

FIG. 1. Logarithmic plot of the absolute errors of the energies obtained for the MPPT series for the five test examples.

from the FCI energies as a function of the perturbation order. The table contains information about the recovered fractions of the full correlation energies for orders up to 6, whether a series converges or diverges, and the archetype as well as sign pattern of the corrections. For convergent series, the rate of convergence is also reported. This template for the figures and tables will also be used in our later discussions of the convergence of the CP energy series.

With respect to the lower-order behavior of the MPPT series, Table II shows that the second-order correlation energy gives more than 93% of the full correlation energy for all examples except for the methylene molecule, where the second-order correlation energy is only about 80% of the full correlation energy. Addition of the third-order correction improves the accuracy of the correlation for the methylene molecule but leads to reduced or only minor improvements for the remaining cases. The inclusion of the fourth-order corrections leads to significant improvements in the accuracy for all cases except the fluorine anion, whereas corrections beyond fourth order do not lead to improvements of the correlation energies, except for the methylene molecule.

Although the two-state model, summarized in Sec. IV B and developed in Ref. 16, is intended to describe the behavior for the higher-order corrections, it may also be used to understand the relative size of the second- and third-order corrections as these corrections may be obtained from a two-state model with the unperturbed reference state and the normalized first-order wave function corrections as the two states. However, the positive second- and third-order MPPT deviations given in Table II do not seem to follow any of the archetypes of the two-state model. To understand why this happens, let us consider the calculation for HF molecule at 1.5 R_e. From the zeroth-order Hamiltonian and the perturbation in the considered two-dimensional space, one obtains a ratio $|\frac{\delta}{\gamma}| = 0.02$, which clearly shows that the archetype is geometric. Furthermore, the sign of γ is negative. However, the observed second- and third-order deviations are both positive, in contrast to the alternating sign pattern of the geometric archetype that is predicted for negative gap shifts in accordance with Table I, as discussed in more detail in Ref. 16.

To understand this behavior, it is noted that the converged energy defining the deviation in the two-state model is the lowest eigenvalue of the two-state problem, rather than the FCI energy which is used to define the deviations for the MPPT energies in Table II and Fig. 1. The FCI energy is lower than the two-state eigenvalue. When the FCI energy is used to define the deviations instead of the two-state eigenvalue, this leads to differences between even and odd order deviations. The second-order energy is below the two-state eigenvalue but above the FCI energy, so using a lower FCI energy as the converged energy leads to a positive value for the second-order deviations. The third-order correction is positive in the standard two-state model, so a lowering of the converged energy increases the size of this deviation, which leads to the observed two positive deviations for second- and third-order MPPT and to a third-order deviation that often is larger than the second-order deviation.

The convergence behavior of the third-order MPPT energy that is marginally better or just slightly worse than the second-order MPPT energy is observed in four of the MPPT calculations reported in Fig. 1 and is a well-known feature of MPPT. The failure to obtain an improved description for MP3 compared to MP2 has the same origin as the failure of MP2 and MP3 to give deviations that are in accordance with the two-state model, as outlined above for HF molecule at 1.5 R_e. An exception, where the third-order MPPT leads to an improvement, is CH_2. However, the gap shift for this molecule is positive so corrections are negative and all deviations are positive, so the change in the value of the converged energy does not modify the behavior of the deviations for this case. The observed higher accuracy of the fourth-order energies compared to the fifth-order energies cannot be described using the two-state model as these energies cannot be obtained from the two-state model.

From Table II, it is seen that the MPPT series is convergent only for the methylene molecule, whereas the series diverges for the remaining four molecules. The convergence archetype is geometric (cf. Fig. 1) for all five cases, and the corrections have alternating signs for HF and F^-, whereas all corrections are negative for the methylene molecule. These findings are in agreement with previous results.[7]

As an example of the asymptotic convergence of a convergent MPPT series, we plot in Fig. 2 the logarithm of the absolute deviations of the MPPT energies for CH_2 as a function of the order together with the linear interpolation defined by the rate of convergence. It is noted that, starting from order 6, the asymptotic rate of convergence gives a curve that is well aligned with the actual deviations. For orders lower than 6, the corrections are reduced significantly faster than predicted by the convergence rate. According to Table II, the rate of convergence for the methylene molecule is 0.79, indicating that it takes three orders in the perturbation to reduce the error by a factor of 2 and thereby about 9 orders to reduce the error by an order of magnitude. This is also supported by Fig. 2.

B. Convergence of the S(D-n) series

In Table III and Fig. 3, we give the absolute deviations from the CCSD energies for the various orders of the CPS(D-n) and E-CCS(D-n) expansions for the considered test examples. To avoid cluttering of the curves, the legends of the various graphs are only given for the upper left panel. When the parent state is the CCS

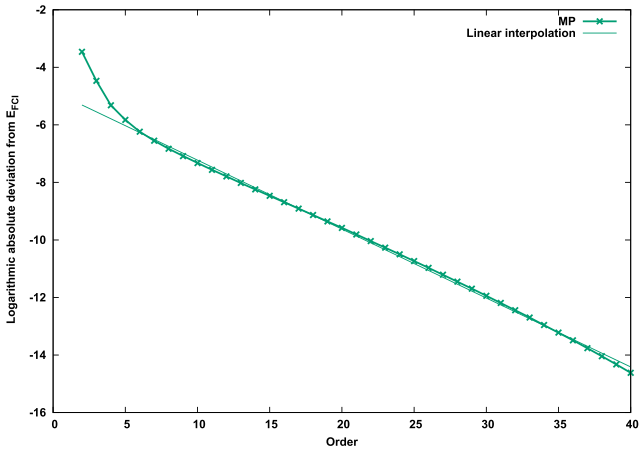

FIG. 2. Logarithmic plot of the absolute errors of the energies obtained for the MPPT calculations on CH_2. The linear least square fit to the points is also given.

TABLE III. Summary of the convergence of the CPS(D-n) calculations.

	HF at R_e	HF at 1.5 R_e	HF at 2 R_e	CH_2	F^-
Low-order results: Fraction of CCSD correlation energy recovered					
Order 2 (%)	98.4	99.0	97.9	84.4	102.3
Order 3 (%)	98.7	97.2	94.6	96.6	98.2
Order 4 (%)	100.5	100.9	101.4	98.7	101.6
Order 5 (%)	99.7	99.3	98.5	99.2	99.0
Order 6 (%)	100.1	100.4	101.1	99.5	100.8
High-order convergence					
Convergent?	Yes	Yes	No	Yes	No
Rate of convergence	0.67	0.83	...	0.68	...
Archetype	Geo.	Geo.	Geo.	Geo.	Geo.
Signs	(1+, 1−)	(1+, 1−)	(1+, 1−)	(−)	(1+, 1−)
Energy/Lagrangian series convergent?	Yes	Yes	No	Yes	Yes

wave function, the reference state is the Hartree-Fock state as the single excitation amplitudes vanish due to the Brillouin theorem. The E-CCS(D-n) and L-CCS(D-n) energy series are therefore identical and equal to the MPPT series with the CCSD wave function as the target state. Figure 3 therefore does not contain an explicit graph for the L-CPS(D-n) series.

From Table III, it is noticed that the second-order energies match the CCSD correlation energies with an error of about 2% or less. An exception is the methylene molecule, where only about 84% of the CCSD correlation energy is recovered at second order. When the third-order corrections are added, it is only for the methylene molecule that a noticeable improvement is observed. The fourth-order corrections give a significant reduction in the deviation, and the CCSD correlation energy is recovered with an error of 0.5% for HF at the equilibrium distance, whereas the deviations are 2% or less for the remaining cases. The next general improvement is now observed at sixth order, where the CCSD correlation energy for all the considered cases is reproduced with an error of 1% or less.

With respect to the convergence behavior for higher-order corrections of the CCS(D-n) series, it is only HF at $2R_e$ and F^-

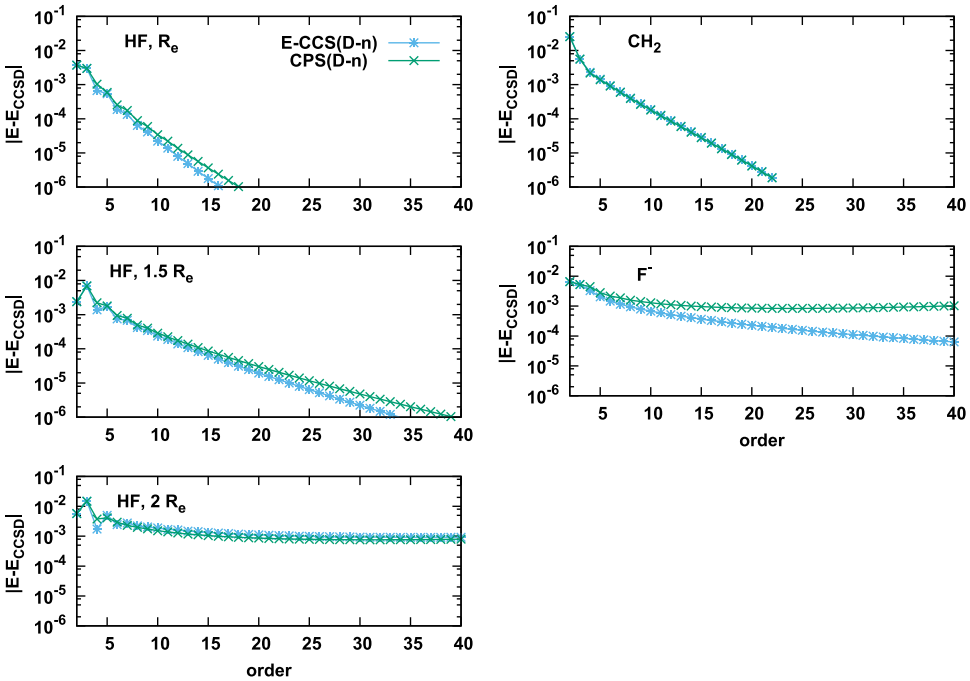

FIG. 3. Logarithmic plot of the absolute errors of the energies obtained in the CPS(D-n) and E-CCS(D-n) series for the five test examples.

that are diverging. The archetype of the convergence is geometric, and the corrections have alternating signs except for the methylene molecule, where all corrections are negative. The archetype patterns in Table I for absolute corrections show that $|\gamma| >> |\delta|$ for all the systems and that $\gamma > 0$ for CH_2, whereas for all other systems $\gamma < 0$. The convergence rates of 0.67 and 0.68 for HF at R_e and CH_2, respectively, indicate fast convergence for these cases, which is also evident from Fig. 3. When HF is stretched to 1.5 R_e, the convergence rate increases to 0.83. When the bond length is stretched to $2R_e$, the series becomes divergent, as already mentioned.

Comparing the results in Table III and Fig. 3 for the CPS(D-n) expansion and the E-CCS(D-n) series, it is seen that both series converge except for HF at $2R_e$ and the fluorine anion. Both series diverge for HF at $2R_e$, whereas only the CPS(D-n) series diverges for the fluorine anion. The divergence of the CPS(D-n) series for the fluorine anion may seem surprising. However, it is noted from Fig. 3 that the E-CCS(D-n) series has a very slow asymptotic convergence, so a small change in the zeroth-order Hamiltonian may change this series to a divergent series. With respect to the convergence rates for the convergent series, it is seen that the convergence of the two series is practically identical for the methylene molecule, whereas the E-CCS(D-n) series converges slightly faster than the CPS(D-n) series for HF at R_e and $1.5R_e$.

C. Convergence of the SD(T-n) series

In the CPSD(T-n) energy series, the zeroth-order parent-space Jacobian contains double excitations and thereby ensures that the largest corrections to the Hartree-Fock state are properly described. The CPSD(T-n) expansion is thus the first CP expansion, where we expect significant improvements in the convergence rates compared to the CCPT energy and CCPT Lagrangian series. Furthermore, in the MPPT, CCPT energy and Lagrangian series front-door intruders are typically dominated by double excitations. By using the full Jacobian in the singles-and-doubles space as the zeroth-order Jacobian, the CPSD(T-n) series can become free of divergences caused by low-lying doubly excited states.

In Table IV, the convergence for the various test cases is summarized in the same form as in Table III for the CPS(D-n) energy series. The table is supplemented by Fig. 4, which gives the absolute errors of the SD(T-n) energies compared to the CCSDT energy. The orders of the L-CCSD(T-n) expansion have been adjusted by adding one order, so their third- and fourth-order corrections equal the third- and fourth-order CPSD(T-n) corrections (see last paragraph of Sec. III).

The third-order corrections are the first non-vanishing corrections, and they give about 90% of the triples correlation energy except for the methylene molecule, where only about 80% of the triples correlation energy is recovered. The fourth-order corrections lead to an improvement only for the methylene molecule. The fifth-order corrections lead to significant improvements of the accuracy, and the triples correlation energies are now recovered for all distances of HF with an error of 0.3% or less, whereas the two remaining test cases exhibit deviations of up to 4%. The sixth-order correction leads to improved accuracy for the methylene molecule only, and the seventh-order terms do not provide a general improvement of the accuracy compared to the fifth-order energies. In the CPSD(T-n) series, we thus again see a pattern, where the first and third non-trivial corrections lead to significant reductions in the deviations, whereas the second and fourth corrections do not provide general improvements.

The third- and fourth-order deviations for all cases, except HF at R_e and methylene, thus show the same behavior as observed for the second- and third-order MPPT deviations. We expect that the reason for the zigzag pattern for these corrections has the same origin as for MPPT. The first non-vanishing correction to the energy is negative and leads to an energy that is lower than that of the corresponding two-state problem. However, the converged CPSD(T-n) energy is below that of the two-state problem and also below that of third order. The use of the CPSDT energy as the reference energy therefore leads to a positive deviation at third order. However, the fourth-order correction is positive and the use of a smaller reference energy leads to an increase in the size of the fourth-order deviation and to the zigzag pattern for low orders.

TABLE IV. Summary of the convergence of the CPSD(T-n) calculations.

	HF at R_e	HF at 1.5 R_e	HF at 2 R_e	CH_2	F^-
Low-order results: Fraction of triples correlation energy recovered					
Order 3 (%)	92.2	90.5	87.6	78.3	93.8
Order 4 (%)	93.4	89.7	87.1	89.0	88.8
Order 5 (%)	99.7	99.9	100.2	95.9	101.5
Order 6 (%)	99.3	98.3	97.3	97.8	97.0
Order 7 (%)	100.1	100.3	100.9	98.9	101.4
High-order convergence					
Convergent?	Yes	Yes	Yes	Yes	Yes
Rate of convergence	0.48	0.57	0.76	0.60	0.74
Archetype	Geo.	Geo.	Geo.	Geo.	Geo.
Signs	(1+, 1−)	(1+, 1−)	(1+, 1−)	(−)	(1+, 1−)
Energy/Lagrangian series convergent?	Yes	Yes	No	Yes	No

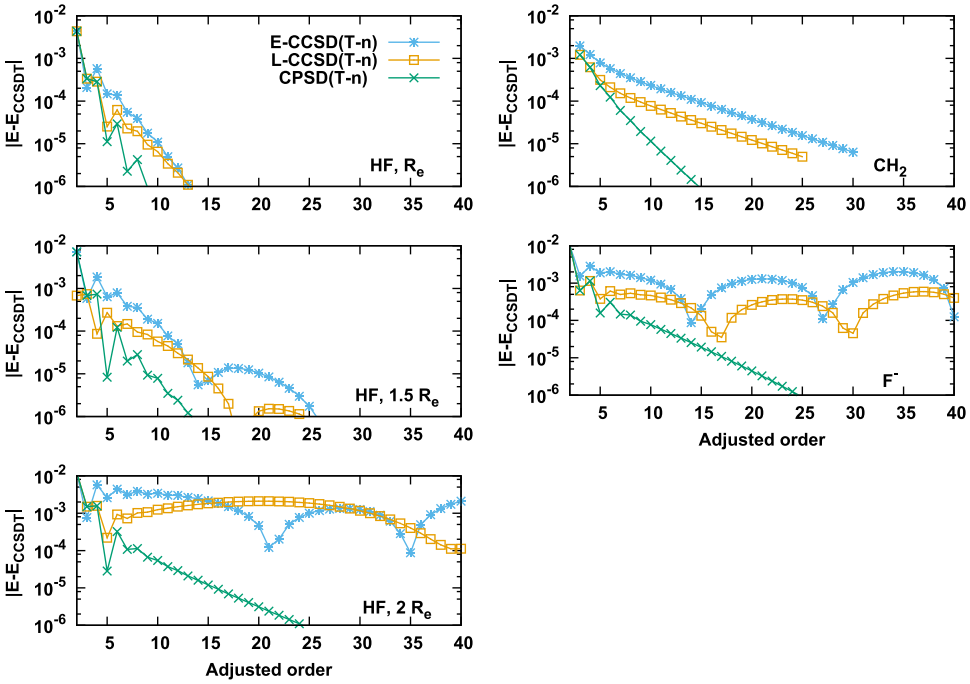

FIG. 4. Energy errors of the three perturbation expansions for CCSD as the parent state and CCSDT as the target state.

Turning to the effect of the higher-order corrections, it is seen from Fig. 4 that the CPSD(T-n) series is convergent for all the considered cases. The archetype for the high-order convergence is again the geometric type with alternating signs for all cases except methylene, where all corrections are negative. The archetype patterns in Table I for absolute corrections show that $|\gamma| >> |\delta|$ for all the systems and that $\gamma > 0$ for CH_2, whereas for all other systems $\gamma < 0$. With convergence rates of 0.48 and 0.57, the CPSD(T-n) series for hydrogen fluoride molecule at R_e and $1.5R_e$, respectively, are well convergent and the convergence rate of 0.76 for the bond stretched to $2.0R_e$ is also encouraging.

For the CCPT energy and Lagrangian series,[9,11] convergence is observed for HF at R_e and $1.5R_e$ and for methylene. The archetype of these series is ripple (see Table I) for HF at the two stretched geometries and for the fluorine anion. The energy corrections within a ripple have alternate sign, and from Table I, we therefore know that the gap shift is negative. From Table I, it is also seen that the period of the ripples is proportional to the ratio between the gap shift and the coupling constant, so the presence of these ripples indicates that the coupling is not much smaller than the gap shift. This may be understood by noting that the CCPT series have a rather inaccurate zeroth-order Jacobian defined by the Fock operator, and therefore large gap shifts and coupling terms occur in these perturbation series.

Comparing the CPSD(T-n) and L-CCSD(T-n) series, we note from Fig. 4 that the first two orders are identical, in agreement with the analysis in Sec. III B. For the fifth, sixth, and seventh order, the CPSD(T-n) expansion gives significantly better results than the CCPT Lagrangian expansion. For higher orders, it is seen that the CPSD(T-n) deviations diminish fast in a geometric fashion, whereas the CCSD(T-n) series exhibits ripples for three test cases and diverges for two cases.

For a more detailed comparison of the performance of the CPSD(T-n) expansion with the CCPT energy and CCPT Lagrangian series, we give in Fig. 5 the signed errors for the three expansions for HF at R_e. It is noted that the E-CCSD(T-n) expansion has errors that are significantly larger than the two other expansions, especially at the lower orders. With the adjusted orders (see last paragraph of Sec. III B), the CPSD(T-n) and L-CCSD(T-n) expansions are identical at third and fourth order, but already from fifth order, the CPSD(T-n) expansion shows much smaller errors: at fifth order, the

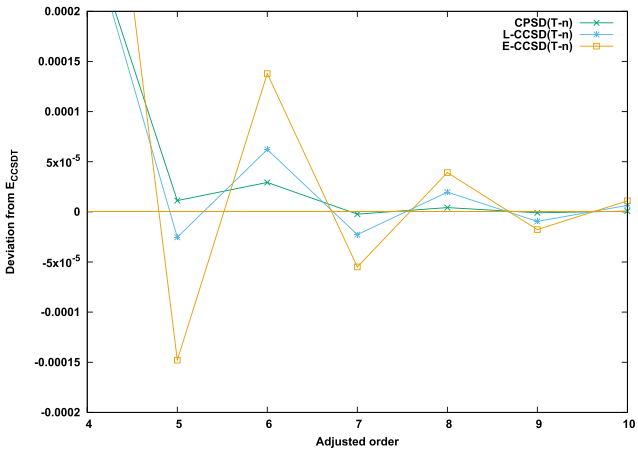

FIG. 5. Convergence of the CCPT energy, CCPT Lagrangian, and CP series with CCSD as the parent state and CCSDT as the target state for HF at R_e.

TABLE V. Summary of the convergence of the CPSDT(Q-n) calculations.

	HF at R_e	HF at 1.5 R_e	HF at 2 R_e	CH_2	F^-
Low-order results: Fraction of quadruples correlation energy recovered					
Order 3 (%)	88.7	89.5	89.8	55.4	71.5
Order 4 (%)	102.9	103.6	103.1	86.9	111.5
Order 5 (%)	99.2	98.6	98.1	94.1	95.9
Order 6 (%)	100.7	101.5	102.3	97.6	102.0
Order 7 (%)	99.8	99.5	98.9	98.9	99.9
High-order convergence					
Convergent?	Yes	Yes	Yes	Yes	Yes
Rate of convergence	0.59	0.64	0.76	0.46	...
Convergence behavior	Geo.	Geo.	Geo.	Geo.	Ripples
Signs	(1+, 1−)	(1+, 1−)	(1+, 1−)	(−)	(1+, 1−)
Energy/Lagrangian series convergent?	Yes	No	No	Yes	No

CPSD(T-n) expansion has an error that is less than half of that of the L-CCSD(T-n) expansion, at sixth order both schemes give increased errors, and from the seventh order, the CPSD(T-n) expansion is converged on the scale of the figure, whereas the L-CCSD(T-n) expansion oscillates around the exact energy.

D. Convergence of the SDT(Q-n) series

The results of calculations for the CPSDT(Q-n) series are given in Table V and in Fig. 6. There are a few practical aspects that must be noted for these calculations. Most importantly, the allowed maximal order was lowered to reduce the timings for these calculations. The low maximal order implies that our identifications of whether a given series is divergent or convergent is on less solid ground than for the calculations presented in Subsections V A–V C. Furthermore, the rate of convergence was obtained using orders 5-10, which makes these rates less accurate.

The first non-trivial corrections, the third-order corrections, recover about 90% of the quadruples correlation energies for HF at the three inter-nuclear distances but only about 50% for methylene

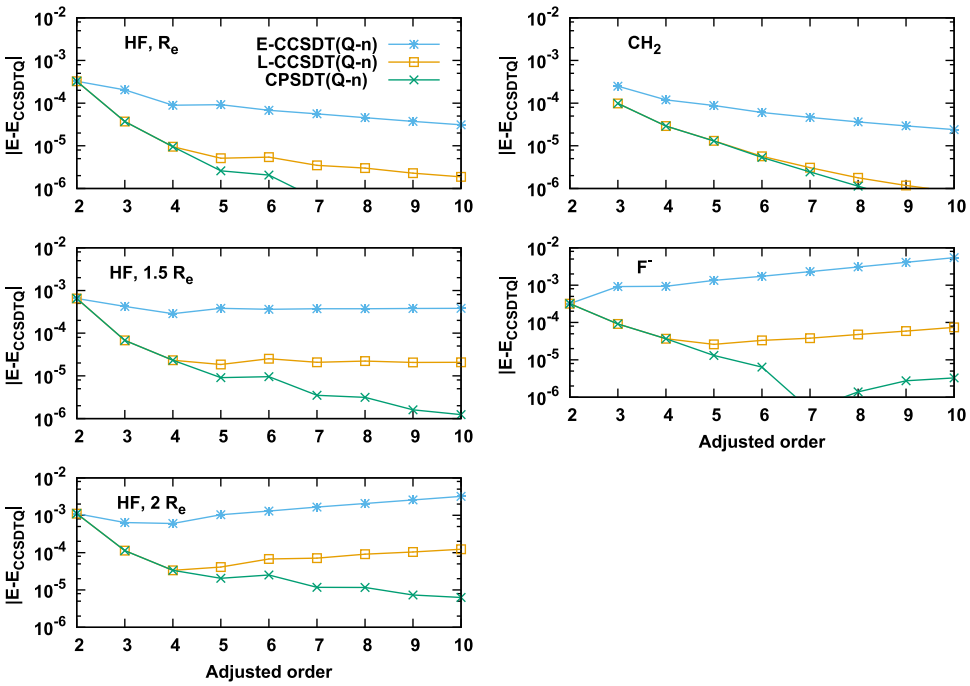

FIG. 6. Energy errors of the three perturbation expansions with CCSDT as the parent state and CCSDTQ as the target state.

and 70% for F^-. The fourth-order corrections improve the accuracy for all five cases, and the deviations are reduced to about 3% for the three calculations on HF. Also the fifth-order corrections improve the accuracy for all five cases, whereas the sixth-order corrections do not give general improvements. Finally, at seventh order, the quadruples correlation energies are recovered with an error of about 1% or less for all five cases.

With the above caveats, the CPSDT(Q-n) series is seen from the figure to converge for all examples. The convergence for fluorine anion is of the ripple archetype, whereas the remaining four cases have the geometric archetype. Due to the occurrence of the ripples for the fluorine anion, we do not give a rate of convergence in the table for this calculation. It also noted from the figure that the CCPT energy and CCPT Lagrangian series at the stretched geometries are both diverging. For the methylene molecule, the CCPT energy expansion is again significantly slower converging than the two other expansions, whereas the L-CCSDT(Q-n) and CPSDT(Q-n) series are very similar up to order six, from where the CCPT Lagrangian expansion converges slowly.

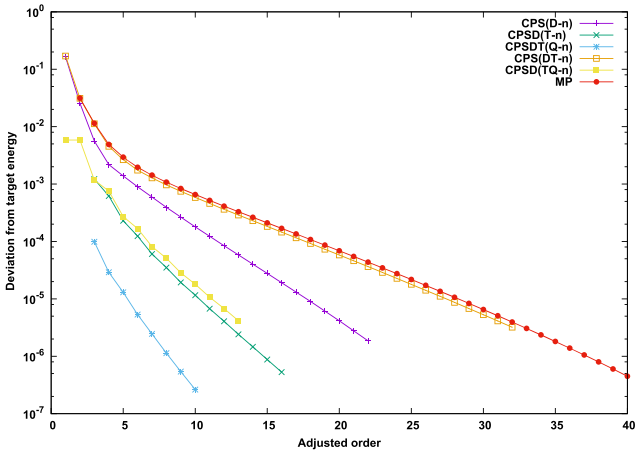

FIG. 7. Deviations from target energies for the CP series and for MPPT for the CH_2 molecule.

E. Comparison of the convergence of the hierarchies

We will now complement the preceding discussions for particular parent and target excitation spaces with a discussion of how the convergence of the CP series changes as a function of the parent and target excitation spaces. Specifically, we will compare the convergence of the various CP series for CH_2 and HF at the equilibrium geometry. For comparison, the MPPT energies will also be discussed.

We start with some general considerations concerning the convergence of the various CP models. When the excitation levels of both the parent and target states are increased, say from the CPS(D-n) to the CPSD(T-n) series, there are two features that must be considered to understand the change in the convergence rate. When the excitation level of the parent state is increased, the part of the Jacobian that is calculated using the exact Hamiltonian is increased, which in general will lead to improved convergence. On the other hand, an increase in the target excitation space may introduce low-lying excited states with a high excitation rank, thereby impairing the convergence of the series. An increase in excitation level for the target space therefore typically impairs the convergence rate, and this will be especially pronounced for systems containing electron-rich atoms.

To examine a case without intruder states in the FCI target space, we first consider the methylene molecule. In Fig. 7, we report the errors of the CP and MPPT series. The errors are relative to the target energy of each expansion, so a small error does not in general indicate a small error compared to the FCI energy.

Consider first how the convergence changes when the target excitation level is increased for a fixed parent excitation level. There are three expansions that have the HF state as the parent state: CPS(D-n), CPS(DT-n), and MPPT. This sequence of the three expansions corresponds to increasing the target excitation space, and we therefore expect that the rate of convergence will decrease as we go from the first to the last of these expansions. This trend is observed in Fig. 7. It is interesting to note that the CPS(DT-n) and MPPT expansions have nearly the same rate of convergence and errors compared to their target states. The errors in the higher orders of the MPPT series are therefore here connected with doubles and triples excitations in the coupled cluster expansion. For the next level of parent excitations, CCSD, it is noted that the rate of convergence is only slightly increased when going from the CPSD(T-n) to the CPSD(TQ-n) series, showing that quadruple excitations are of limited importance for the convergence. When the parent excitation level is changed without changing the maximum target excitation level, as is the case when comparing the CPS(DT-n) with CPSD(T-n) and CPSD(TQ-n) with CPSDT(Q-n), it is noted that both the initial errors and the convergence rates are reduced significantly, in line with our expectations.

When both the parent and target excitation levels are increased, lower initial errors and faster convergence are observed. This is evident from Fig. 7 and is supported by the convergence rates which in Tables III–V are listed as 0.68, 0.60, and 0.48 for CPS(D-n), CPSD(T-n), and CPSDT(Q-n) expansions, respectively.

To see how back-door intruders or near back-door intruders affect the convergence, we give in Fig. 8 the absolute errors for the CP and MPPT series for HF at R_e. Due to the presence of a back-door intruder state that is dominated by triple and higher excitations, we expect that the rate of convergence is very dependent on the target state. Thus, the full MPPT expansion is diverging in contrast to the CPS(DT-n) expansion, which is converging slower than the CPS(D-n) expansion. When the parent excitation level is increased for a fixed target state, it is seen that the rate of convergence is increased as expected, both when going from the CPS(DT-n) to the CPSD(T-n) series and from the CPSD(TQ-n) to the CPSDT(Q-n) series. When the excitation levels of both the parent space and target space are increased, the effect on the convergence rate depends on the maximal excitation level in the target space. Thus, when going from the CPS(D-n) to the CPSD(T-n), the convergence is significantly improved, but when going from the CPSD(T-n) to the CPSDT(Q-n), it is observed that the CPSDT(Q-n) series is slower converging. In this case, the enlargement of the target excitation space slows the convergence more down than the enlargement of the parent excitation space improves the convergence.

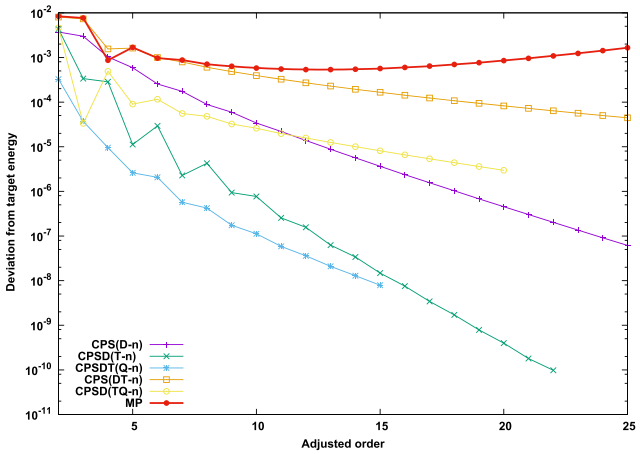

FIG. 8. Deviations from target energies for the CP series and for MPPT for the HF molecule at R_e.

F. Summary of the numerical results

For parent states beyond the trivial CCS state, the CP models exhibit in general superior convergence behavior compared to the CCPT energy and CCPT Lagrangian series, both with respect to the accuracy of the lower order results and the convergence or divergence of the higher-order contributions. Comparing specifically the CCPT Lagrangian and the CP series for parent states beyond CCS, and using adjusted orders, the third- and fourth-order results are identical, whereas the fifth-order CP energies are noticeably more accurate than their CCPT Lagrangian counterparts. For example, at the SD(T-n) level of theory, the fifth-order energy for hydrogen fluoride at the equilibrium geometry gives 99.7% of the triples correlation energy for the CPSD(T-n) model and 100.6% for the L-CCSD(T-n) model. For systems such as methylene, without back-door intruder states dominated by triple and higher excitation levels, a simultaneous increase in the excitation levels of the parent and target state leads not only to reduced errors of the initial energies but also to faster convergence of the CP series. For molecules such as hydrogen fluoride, containing back-door intruders dominated by high excitations levels, the change in the convergence behavior depends on the balance between two effects: the increase in the parent excitation space leads to an improvement of the convergence, whereas the increase in the target excitation space leads to a degradation of the convergence. Without a thorough investigation, it is therefore not possible to predict the change in the convergence rate when the excitation levels are increased for both the parent and the target excitation spaces. Figure 8 shows that for hydrogen fluoride at R_e, the convergence improves when going from CPS(D-n) to CPSD(T-n) but deteriorates when going from CPSD(T-n) to CPSDT(Q-n). With respect to the question of convergence or divergence, the CP models may converge for molecules where both the MPPT and CCPT Lagrangian series diverge. For example, the CP models converge and the MPPT expansion diverges for hydrogen fluoride at the equilibrium geometry when basis sets containing diffuse function are used.

VI. SUMMARY AND CONCLUSION

We have developed the cluster perturbation (CP) model, in which perturbation theory is used to calculate the energy and molecular properties of the ground and excited states and transition molecular properties between these states, including excitation energies. In the CP models, we consider a target excitation space that is partitioned into a parent and an auxiliary excitation space and determine perturbation series in orders of the CC parent-state similarity-transformed fluctuation potential, where the zeroth-order contribution in the series is the energy or molecular property of the CC parent state and where the perturbation series formally converge to the energy or molecular property of the CC target state.

In conventional Møller-Plesset perturbation theory,[1] the Hamiltonian is partitioned into a Fock operator and a fluctuation potential and the Schrödinger equation is solved in orders of the fluctuation potential collecting terms strictly as zeroth-order Fock operator contributions and first-order fluctuation potential contributions. The CCPT series were derived[9,11] using this strategy and therefore contain contributions that originate from internal relaxation in the parent excitation space. In CP theory, we have introduced a generalized order concept, where the zeroth-order component of the extended CC parent-state Jacobian contains in the parent excitation space a fluctuation potential contribution, and we have used this generalization of the order concept to turn internal relaxation in the parent excitation space into a zeroth-order effect. Since internal relaxation in the parent excitation space in general is large, compared to the effect of introducing an auxiliary excitation space, the generalized order concept results in greatly improved local and global convergence of the CP energy series compared to the CCPT series. At the same time, the generalization of the order concept does *not* increase the leading-order computational scaling compared to the CCPT series. Most importantly, however, the generalized order concept of CP theory also makes it possible to determine perturbation expansions for molecular properties where the zeroth-order molecular property is the molecular property of the CC parent state and the perturbation series converge to the molecular property for the CC target state. We have shown in this paper that CP perturbation series exist for molecular properties. We have thus developed a perturbation framework where perturbation series for the energy and for molecular properties can be determined on an equal footing. A detailed derivation of CP perturbation series for molecular properties, including excitation energies, is deferred to future work.

In CP theory, we do not need to solve amplitude and response equations in the target space explicitly. The perturbation series in general show fast local convergence toward the CC target state energies and molecular properties, and it therefore becomes computationally very tractable to use low-order corrections from the perturbation series to obtain energies and molecular properties of CC target-state quality.

In this paper, we have illustrated with numerical examples the convergence of the perturbation series for the energy for various parent and target excitation spaces. For the energy series CPS(D-n), where the parent excitation space contains only singles and the auxiliary excitation space contains doubles, the convergence of the CPS(D-n) energy series is not improved compared to the CCPT series[9,11] since internal relaxation effects in the singles excitation

space are of minor importance compared to introducing a doubles auxiliary space. However, the CPS(D-n) series is important as it may be used to determine series for molecular properties, including excitation energies, as opposed to the CCPT series that can only be used to obtain series for the energy. For the CP energy series where the parent space contain at least a singles-and-doubles excitation space and where the auxiliary space contains only one excitation level, internal relaxation in the parent excitation space is large and the CP energy series exhibit a greatly improved convergence compared to the CCPT series.

The convergence of CP series in general improves when the parent excitation space is increased. This is in accordance with our physical understanding as an increase in the parent excitation space leads to an improved description of the zeroth-order state, i.e., the CC parent state, and the perturbation series therefore becomes less plagued by front-door intruders that are states strongly interacting with the zeroth-order state. The convergence of CP series also improves when decreasing the size of the auxiliary excitation space. This is a more surprising finding. Its origin is that by reducing the excitation level of the auxiliary space, the existence of back-door intruders becomes less likely as back-door intruders are highly lying excited states that are nearly independent of the physical perturbation.

We have focused on using CP series where the auxiliary space contains only one excitation level, both to have fast convergent perturbation series and because too much effort, in general, is spent on optimizing amplitudes at the highest excitation level for amplitudes that are far from converged at the lower excitation level if the auxiliary space contains more than one excitation level.

The applicability of CP theory to both the energy and molecular properties and numerical results for CP energy series have demonstrated the superiority of CP theory compared to previous perturbation models, and low-order corrections in the CP perturbation series may be expected soon to become the state-of-the-art electronic structure models for determination of energies and molecular properties including excitation energies of target-state quality for single-configuration dominated molecular systems.

ACKNOWLEDGMENTS

F.P. acknowledges the qLEAP Center for Theoretical Chemistry, Department of Chemistry, Aarhus University, Langelandsgade 140, DK-8000 Aarhus C, Denmark, where he was formerly employed and where research leading to this article was carried out. F.P. and P.J. acknowledge support from the European Research Council under the European Union's (EU) Seventh Framework Programme (No. FP/2007-2013)/ERC Grant Agreement No. 291371. J.O. acknowledges support from the Danish Council for Independent Research, Grant No. DFF-4181-00537.

REFERENCES

[1] C. Møller and M. S. Plesset, Phys. Rev. **46**, 618 (1934).
[2] D. Cremer, Wiley Interdiscip. Rev.: Comput. Mol. Sci. **1**, 509 (2011).
[3] N. C. Handy, R. D. Amos, J. F. Gaw, J. E. Rice, and E. D. Simandiras, Chem. Phys. Lett. **120**, 151 (1985).
[4] E. D. Simandiras, R. D. Amos, and N. C. Handy, Chem. Phys. **114**, 9 (1987).
[5] J. A. Pople, R. Krishnan, H. B. Schlegel, and J. S. Binkley, Int. J. Quantum Chem. **S13**, 225 (1979).
[6] D. H. Friese, N. O. C. Winter, P. Balzerowski, R. Schwan, and C. Hättig, J. Chem. Phys. **136**, 174106 (2012).
[7] J. Olsen, O. Christiansen, H. Koch, and P. Jørgensen, J. Chem. Phys. **105**, 5082 (1996).
[8] T. Helgaker, P. Jørgensen, and J. Olsen, *Molecular Electronic-Structure Theory* (Wiley, Chichester, 2000).
[9] J. J. Eriksen, K. Kristensen, T. Kjærgaard, P. Jørgensen, and J. Gauss, J. Chem. Phys. **140**, 064108 (2014).
[10] J. J. Eriksen, P. Jørgensen, and J. Gauss, J. Chem. Phys. **142**, 014102 (2015).
[11] K. Kristensen, J. J. Eriksen, D. A. Matthews, J. Olsen, and P. Jørgensen, J. Chem. Phys. **144**, 064103 (2016).
[12] F. Pawłowski, J. Olsen, and P. Jørgensen, "Cluster perturbation theory. V. Theoretical foundation for cluster linear target states," J. Chem. Phys. **150**, 134112 (2019).
[13] O. Christiansen, J. Olsen, P. Jørgensen, H. Koch, and P.-Å. Malmqvist, Chem. Phys. Lett. **261**, 369 (1996).
[14] J. J. Eriksen, K. Kristensen, D. A. Matthews, P. Jørgensen, and J. Olsen, J. Chem. Phys. **145**, 224104 (2016).
[15] F. Pawłowski, J. Olsen, and P. Jørgensen, "Cluster perturbation theory. IV. Convergence of cluster perturbation series for energies and molecular properties," J. Chem. Phys. **150**, 134111 (2019).
[16] J. Olsen and P. Jørgensen, "Convergence patterns and rates in two-state perturbation expansions," J. Chem. Phys. (submitted).
[17] S. Hirata, M. Nooijen, I. Grabowski, and R. J. Bartlett, J. Chem. Phys. **114**, 3919 (2001).
[18] S. Hirata, P.-D. Fan, A. A. Auer, M. Nooijen, and P. Piecuch, J. Chem. Phys. **121**, 12197 (2004).
[19] T. Shiozaki, K. Hirao, and S. Hirata, J. Chem. Phys. **126**, 244106 (2007).
[20] S. R. Gwaltney and M. Head-Gordon, Chem. Phys. Lett. **323**, 21 (2000).
[21] S. R. Gwaltney and M. Head-Gordon, J. Chem. Phys. **115**, 2014 (2001).
[22] K. Kowalski and P. Piecuch, J. Chem. Phys. **113**, 18 (2000).
[23] P. Piecuch and M. Włoch, J. Chem. Phys. **123**, 224105 (2005).
[24] P. Piecuch, M. Włoch, J. R. Gour, and A. Kinal, Chem. Phys. Lett. **418**, 467 (2006).
[25] J. F. Stanton and R. J. Bartlett, J. Chem. Phys. **98**, 7029 (1993).
[26] S. Coriani, F. Pawłowski, J. Olsen, and P. Jørgensen, J. Chem. Phys. **144**, 024102 (2016).
[27] I. Shavitt and R. J. Bartlett, *Many-Body Methods in Chemistry and Physics: MBPT and Coupled-Cluster Theory* (Cambridge University Press, 2009).
[28] H. Koch and P. Jørgensen, J. Chem. Phys. **93**, 3333 (1990).
[29] N. C. Handy, P. J. Knowles, and K. Somasundram, Theor. Chem. Acc. **68**, 87 (1985).
[30] J. Olsen, P. Jørgensen, T. Helgaker, and O. Christiansen, J. Chem. Phys. **112**, 9736 (2000).
[31] J. Olsen, J. Chem. Phys. **113**, 7140 (2000).
[32] J. Olsen, Lucia—a configuration interaction and coupled cluster program, University of Aarhus, 2016.
[33] K. Aidas, C. Angeli, K. L. Bak, V. Bakken, R. Bast, L. Boman, O. Christiansen, R. Cimiraglia, S. Coriani, P. Dahle, E. K. Dalskov, U. Ekström, T. Enevoldsen, J. J. Eriksen, P. Ettenhuber, B. Fernández, L. Ferrighi, H. Fliegl, L. Frediani, K. Hald, A. Halkier, C. Hättig, H. Heiberg, T. Helgaker, A. C. Hennum, H. Hettema, E. Hjertenæs, S. Høst, I.-M. Høyvik, M. F. Iozzi, B. Jansík, H. J. A. Jensen, D. Jonsson, P. Jørgensen, J. Kauczor, S. Kirpekar, T. Kjærgaard, W. Klopper, S. Knecht, R. Kobayashi, H. Koch, J. Kongsted, A. Krapp, K. Kristensen, A. Ligabue, O. B. Lutnæs, J. I. Melo, K. V. Mikkelsen, R. H. Myhre, C. Neiss, C. B. Nielsen, P. Norman, J. Olsen, J. M. H. Olsen, A. Osted, M. J. Packer, F. Pawłowski, T. B. Pedersen, P. F. Provasi, S. Reine, Z. Rinkevicius, T. A. Ruden, K. Ruud, V. V. Rybkin, P. Sałek, C. C. M. Samson, A. Sánchez de Merás, T. Saue, S. P. A. Sauer, B. Schimmelpfennig, K. Sneskov, A. H. Steindal, K. O. Sylvester-Hvid, P. R. Taylor, A. M. Teale, E. I. Tellgren, D. P. Tew, A. J. Thorvaldsen, L. Thøgersen, O. Vahtras, M. A. Watson, D. J. D. Wilson, M. Ziółkowski, and H. Ågren, Wiley Interdiscip. Rev.: Comput. Mol. Sci. **4**, 269 (2014).
[34] See http://daltonprogram.org/ for dalton, a Molecular Electronic Structure Program, Release DALTON2016.1, 2016.